Model-Based Meta-Analysis to Optimize *Staphylococcus aureus*–Targeted Therapies for Atopic Dermatitis

Takuya Miyano[1], Alan D. Irvine[2,3] and Reiko J. Tanaka[1]

Several clinical trials of *Staphylococcus aureus* (*S. aureus*)–targeted therapies for atopic dermatitis (AD) have shown conflicting results about whether they improve AD severity scores. This study performs a model-based meta-analysis to investigate the possible causes of these conflicting results and suggests how to improve the efficacies of *S. aureus*–targeted therapies. We developed a mathematical model that describes systems-level AD pathogenesis involving dynamic interactions between *S. aureus* and coagulase-negative *Staphylococcus* (CoNS). Our model simulation reproduced the clinically observed detrimental effects of the application of *S. hominis* A9 and flucloxacillin on AD severity and showed that these effects disappeared if the bactericidal activity against CoNS was removed. A hypothetical (modeled) eradication of *S. aureus* by 3.0 $\log_{10}$ colony-forming unit per cm^2 without killing CoNS achieved Eczema Area and Severity Index 75 comparable with that of dupilumab. This efficacy was potentiated if dupilumab was administered in conjunction with *S. aureus* eradication (Eczema Area and Severity Index 75 at week 16) (*S. aureus* eradication: 66.7%, dupilumab 61.6% and combination 87.8%). The improved efficacy was also seen for virtual dupilumab poor responders. Our model simulation suggests that killing CoNS worsens AD severity and that *S. aureus*–specific eradication without killing CoNS could be effective for patients with AD, including dupilumab poor responders. This study will contribute to designing promising *S. aureus*–targeted therapy.

JID Innovations (2022);**2:**100110 doi:10.1016/j.xjidi.2022.100110

INTRODUCTION

Atopic dermatitis (AD), also called eczema, is the most common inflammatory skin disease (Deckers et al., 2012). The symptoms of AD involve relapsing pruritus and skin pain, which impairs patients' QOL and work productivity (Simpson et al., 2016a). The pathogenesis of AD is characterized by skin barrier damage, T helper 2–dominant inflammation, and skin dysbiosis (Czarnowicki et al., 2019; Langan et al., 2020; Weidinger et al., 2018). The most well-understood skin dysbiosis in patients with AD is colonization by *Staphylococcus aureus* and a decreased relative abundance of commensal bacteria in the skin (Ederveen et al., 2019). *S. aureus* skin colonization is found in 75–90% of patients with AD without clinical signs of superinfection, whereas it is found in only 0–25% of healthy subjects (Breuer et al., 2002; Gong et al., 2006; Higaki et al., 1999; Nath et al., 2020; Park et al., 2013).

[1]*Department of Bioengineering, Imperial College London, London, United Kingdom;* [2]*Pediatric Dermatology, Children's Health Ireland at Crumlin, Dublin, Ireland; and* [3]*Clinical Medicine, College of Medicine, Trinity College Dublin, The University of Dublin, Dublin, Ireland*

Correspondence: Reiko J. Tanaka, Department of Bioengineering, Imperial College London, South Kensington Campus, London SW7 2AZ, United Kingdom. E-mail: r.tanaka@imperial.ac.uk

Abbreviations: AD, atopic dermatitis; agr, accessory gene regulatory; AIP, autoinducing peptide; AMP, antimicrobial peptide; CoNS, coagulase-negative Staphylococcus; EASI, Eczema Area and Severity Index; QSP, quantitative systems pharmacology; Sh*A9,* Staphyloccocus hominis *A9*

Received 18 October 2021; revised 18 January 2022; accepted 25 January 2022; accepted manuscript published online 18 February 2022; corrected proof published online 19 May 2022

Cite this article as: JID Innovations 2022;2:100110

S. aureus colonization density correlates with AD severity (Callewaert et al., 2020; Cau et al., 2021), and *S. aureus* has been considered a promising target for AD treatment because it induces both skin barrier damage and inflammation by producing various virulence factors, such as phenol-soluble modulins, staphylococcal enterotoxins, and the toxic shock syndrome toxin-1 (Geoghegan et al., 2018; Syed et al., 2015).

Some clinical trials of *S. aureus*–targeted therapies for AD have indeed shown a reduction in *S. aureus* densities (Tham et al., 2020). However, they have shown conflicting results as to whether they improve AD severity scores. For example, in several clinical trials, oral and topical antistaphylococcal antibiotics were applied to eradicate *S. aureus* at least temporarily on AD skin lesions. However, these interventions often failed to improve AD severity. A Cochrane review concluded that antibiotics may make no difference or only a slight improvement in AD severity (George et al., 2019). Oral flucloxacillin, one of the antibiotics, worsened AD severity than placebo, despite a significant reduction of *S. aureus* levels on skin lesions (Ewing et al., 1998). Currently, the use of antibiotics is recommended for AD only in case of overt infection (Alexander et al., 2020; LePoidevin et al., 2019).

As another *S. aureus*–targeted therapy, transplantation of *S. hominis* A9 (*Sh*A9), a commensal strain of coagulase-negative staphylococci (CoNS) isolated from healthy human skin, has been tested (Nakatsuji et al., 2021a). A clinical study showed that *Sh*A9 transplantation decreased the *S. aureus* levels on skin lesions and improved AD severity scores in the patients (n = 21) whose skin was colonized with *S. aureus* that is sensitive to the bacteriocins secreted by *Sh*A9. However, the *Sh*A9 transplantation worsened AD

severity scores in patients (n = 11) whose skin was colonized with *S. aureus* resistant to the bacteriocins secreted by *Sh*A9 (Nakatsuji et al., 2021a). *Sh*A9 produces bacteriocins with bactericidal activity against *S. aureus* (Nakatsuji et al., 2017) and secretes autoinducing peptides (AIPs) that inhibit the accessory gene regulatory (agr) system, which regulates the expression of the virulence factors in *S. aureus* (Williams et al., 2019).

Some therapeutics that do not target *S. aureus* directly can also reduce *S. aureus* levels. Dupilumab, an approved biologic for AD, is a mAb that inhibits IL-4 and IL-13 signaling. These T helper 2 cytokines can facilitate *S. aureus* colonization because they damage the skin barrier by inhibiting epidermal differentiation (Howell et al., 2009; Seltmann et al., 2015); skin barrier damage induces an increase in skin pH (Elias, 2017) that promotes *S. aureus* growth (Lambers et al., 2006). In addition, inhibition of IL-4 and IL-13 by dupilumab can reduce *S. aureus* levels because IL-4 and IL-13 inhibit the synthesis of antimicrobial peptides (AMPs) against *S. aureus* (Howell et al., 2006). Dupilumab has been shown to reduce *S. aureus* levels and improve AD severity scores in a clinical trial (Callewaert et al., 2020).

Taken together, flucloxacillin, *Sh*A9, and dupilumab decreased *S. aureus* levels but showed contrasting efficacies with respect to improved AD severity scores. Understanding the underlying mechanism for these contrasting efficacies will help to optimize consistently effective *S. aureus*–targeted therapies for AD.

To investigate the causes of the conflicting efficacies of *S. aureus*–targeted therapies, this study applies a quantitative systems pharmacology (QSP) approach. QSP is a framework to describe systems-level pathogenesis and treatment effects by integrating data and knowledge into a mathematical model (Schoeberl, 2019). A QSP approach facilitates a model-based meta-analysis that integrates data from different clinical trials as well as knowledge on pathogenesis and mechanism of action of treatments to inform rational drug development (Gibbs et al., 2018). A QSP model–based meta-analysis is especially suitable for this study, which aims to investigate the underlying mechanisms for the conflicting efficacies of *S. aureus*–targeted therapies observed in different clinical studies.

We have recently applied a QSP model–based meta-analysis of multiple biologics for AD and identified IL-13 and IL-22 as potential drug targets for dupilumab poor responders (Miyano et al., 2021). However, the previous QSP model of biologics is not suitable for this study's aim because it did not describe the mechanism of *S. aureus*–targeted therapies. This study presents a new QSP model of *S. aureus*–targeted therapies that describes the interactions between *S. aureus* and CoNS in AD pathogenesis by referring to clinical efficacy data of the three treatments described earlier: flucloxacillin, *Sh*A9, and dupilumab. The selection process is detailed in Supplementary Figures S1 and S2, Supplementary Table S1 and "Selection of clinical studies for development of the quantitative systems pharmacology model" in Supplementary Materials and Methods to test the following two hypotheses.

Our first hypothesis is that the bactericidal effects of *S. aureus*–targeted therapies on CoNS impair their efficacies on AD severity. A decrease in CoNS levels causes a reduction in their AIP secretion, thereby upregulating agr expression. Upregulated agr expression promotes the production of virulence factors in *S. aureus* that can worsen AD severity. Although such a hypothesis has already been implied in several studies (Clowry et al., 2019; Katsuyama et al., 2005; Nakatsuji et al., 2021a), to the best of our knowledge, there has been no quantitative evaluation on the possible dynamic influences of killing CoNS on clinical efficacies.

The second hypothesis is that *S. aureus*–targeted therapies are effective for dupilumab poor responders because they have a different mechanism of action from dupilumab. The responder rates for dupilumab were 44–69% (Blauvelt et al., 2017; Simpson et al., 2016b) for Eczema Area and Severity Index (EASI) 75 (75% reduction in the EASI score) (Hanifin et al., 2001; Schram et al., 2012), leaving a significant proportion of dupilumab poor responders. Therapeutic options for dupilumab poor responders are limited to increasing topical corticosteroids and adding additional systemic immunosuppressive agents. However, dupilumab poor responders are often resistant to these treatments and require monitoring for adverse effects (Hendricks et al., 2019), leaving unmet medical needs for dupilumab poor responders. This paper proposes promising *S. aureus*–targeted therapies for patients with AD, especially for dupilumab poor responders, by conducting model simulations on virtual patients.

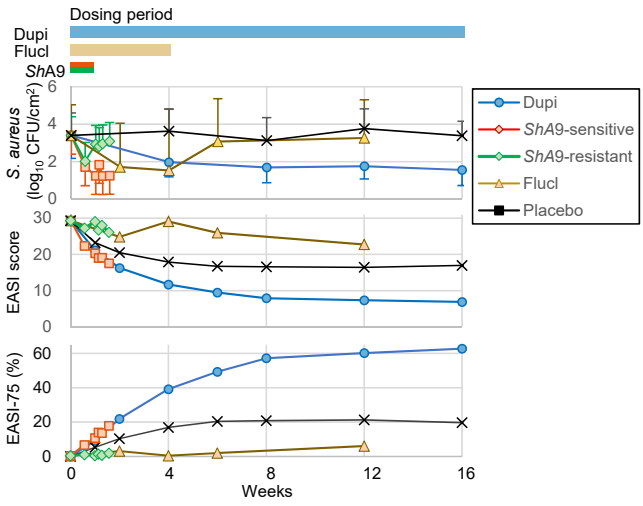

Figure 1. Three treatments (Flucl, *Sh*A9, and Dupi) reduced *Staphylococcus aureus* levels but showed conflicting clinical efficacies regarding EASI scores. *S. aureus* levels, the EASI score, and EASI-75 were normalized using the reported data of each clinical trial ("Data processing" in Supplementary Materials and Methods). For *Sh*A9, we evaluated the efficacies for the patients stratified by whether the colonized *S. aureus* is sensitive to *Sh*A9 bacteriocins (*Sh*A9-sensitive) or is resistant to *Sh*A9 bacteriocins (*Sh*A9-sensitive). Horizontal bars on the top represent the dosing periods in each clinical trial. Error bars denote SD. CFU, colony-forming unit; Dupi, dupilumab; EASI, Eczema Area and Severity Index; Flucl, flucloxacillin; *Sh*A9, *Staphyloccocus hominis* A9.

RESULTS

QSP model reproduced clinical efficacies of three treatments that decreased *S. aureus* levels

We normalized *S. aureus* levels, EASI scores, and EASI-75 using the reported results in clinical trials to compare the

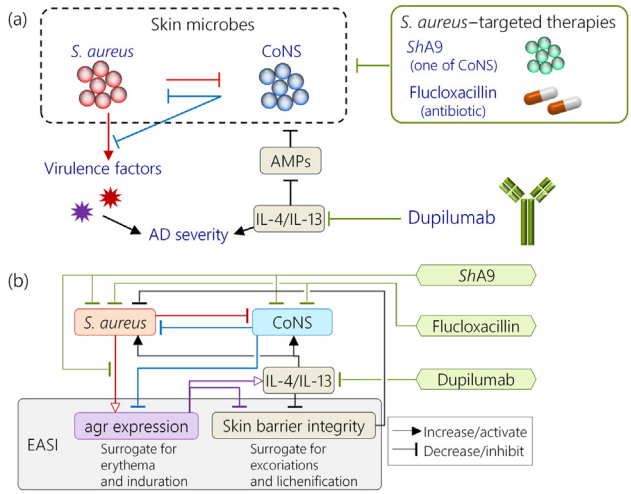

Figure 2. Overview of the QSP model that describes the interactions between *Staphylococcus aureus* and CoNS in AD pathogenesis. (**a**) Schematic diagram. (**b**) Regulatory pathways of the QSP model. The model comprises the EASI score (an efficacy endpoint), skin barrier integrity, agr expression, *S. aureus*, CoNS, IL-4/IL-13, and treatments (*Sh*A9, flucloxacillin, and dupilumab). The regulatory pathways between biological factors are described according to published human data ("Model structure" in Supplementary Materials and Methods). AD, atopic dermatitis; agr, accessory gene regulatory; AMP, antimicrobial peptide; CoNS, coagulase-negative *Staphylococcus*; EASI, Eczema Area and Severity Index; QSP, quantitative systems pharmacology; *Sh*A9, *Staphyloccocus hominis* A9.

efficacies of flucloxacillin, *Sh*A9, and dupilumab (Figure 1, Supplementary Figure S3 and "Data processing" in Supplementary Materials and Methods). Efficacies of *Sh*A9 were presented for two groups of patients stratified by the sensitivity of their *S. aureus* to *Sh*A9 bacteriocins, as in the original clinical study (Nakatsuji et al., 2021a). Hereafter, *Sh*A9 applied to patients colonized with *S. aureus* that is sensitive to *Sh*A9 bacteriocins is referred as *Sh*A9-sensitive, and those with *S. aureus* that is resistant to *Sh*A9 bacteriocins is referred as *Sh*A9-resistant.

The normalized efficacies showed that all the treatments decreased *S. aureus* levels and that *Sh*A9-sensitive and dupilumab improved the EASI scores and EASI-75, whereas *Sh*A9-resistant and flucloxacillin worsened the EASI scores and EASI-75. The results confirmed that the three treatments showed conflicting efficacies on AD severity scores, although they all reduced *S. aureus* levels.

We revised our previously published QSP model of biologics (Miyano et al., 2021) to include the mechanism of action for the three treatments and interactions between *S. aureus* and CoNS (Figure 2, Supplementary Figures S4-S11 and "Model structure" in Supplementary Materials and Methods). The new QSP model of *S. aureus*–targeted therapies reproduced the baseline levels of the biological factors and the clinical efficacies of the treatments on *S. aureus* levels, EASI scores, and EASI-75 (Figure 3a and b, Supplementary Figure S12 and "Optimizing model parameters to reproduce clinical data" in Supplementary Materials and Methods). The root mean square errors of the mean and coefficient of variation of *S. aureus* levels, the EASI scores, and EASI-75 between the simulated and reference data were 0.3 $\log_{10}$ colony-forming units per cm^2 and 43%, 1.5 (of 72, which is the maximal EASI score), and 2.9%, respectively.

Detrimental effects of flucloxacillin and *Sh*A9 on EASI scores disappeared when their bactericidal activity against CoNS was hypothetically removed

Using the new QSP model, we tested the first hypothesis that the bactericidal effects on CoNS impair the efficacies of *S. aureus*–targeted therapies on AD severity. Our model simulation showed that flucloxacillin and *Sh*A9-resistant decreased CoNS while increasing the agr expression (Figure 3c) and that flucloxacillin and *Sh*A9 could achieve better EASI scores and EASI-75 than placebo if they had no bactericidal effects on CoNS (Figure 4). In addition, a sensitivity analysis of the model parameters for percentage-improved EASI score showed that lower rates of CoNS killing by flucloxacillin (d_{fh}) and *Sh*A9 (d_{A9h}) result in a higher percentage-improved EASI score (Supplementary Figure S13 and "Sensitivity analysis" in the Supplementary Materials and Methods). These results suggested that a decrease in CoNS increases agr expression, thereby worsening EASI scores.

Although CoNS levels were reduced to similar levels in both the *Sh*A9-sensitive and *Sh*A9-resistant groups, agr expression was reduced only in the *Sh*A9-sensitive group (Figure 3c). The agr expression decreased because of the stronger decrease of *S. aureus* levels by *Sh*A9-sensitive than by *Sh*A9-resistant, even though the decrease in CoNS resulted in a slight increase in the agr expression. These results suggest that the efficacies of *S. aureus*–targeted therapies are determined in some part by the balance of their bactericidal strengths against *S. aureus* versus CoNS.

Hypothetical *S. aureus*–targeted therapies achieved better EASI-75 than dupilumab

The QSP model described antimicrobial effects of *S. aureus*–targeted therapies by three parameters: the rate of *S. aureus* killing, that of CoNS killing, and the strength of agr expression inhibition (Figure 2). The antimicrobial effects resulted in a decrease of *S. aureus* levels, that of CoNS level, and inhibition of agr expression level, respectively (Figure 5a). To explore which antimicrobial effects are responsible for improvement in AD severity, we conducted model simulations for hypothetical *S. aureus*–targeted therapies with different values of the three parameters.

Our simulation results showed that lower *S. aureus* levels, higher CoNS levels, and stronger inhibition of agr expression resulted in higher EASI-75 after 16 weeks (Figure 5b, left). The *S. aureus*–specific eradication (the maximal reduction of *S. aureus* level without killing CoNS, yellow arrows in Figure 5b) led to comparable EASI-75 with dupilumab (66.7 vs. 61.6% for dupilumab). The EASI-75 of the *S. aureus*–specific eradication was improved by adding 90% inhibition of the agr expression (70.6%, blue arrows in Figure 5b).

Simulations for a combinatorial application of dupilumab and hypothetical *S. aureus*–targeted therapies elucidated that it can achieve better EASI-75 than an application of either one (Figure 5b, right). The *S. aureus*–specific eradication improved EASI-75 (87.8%) when it was combined with

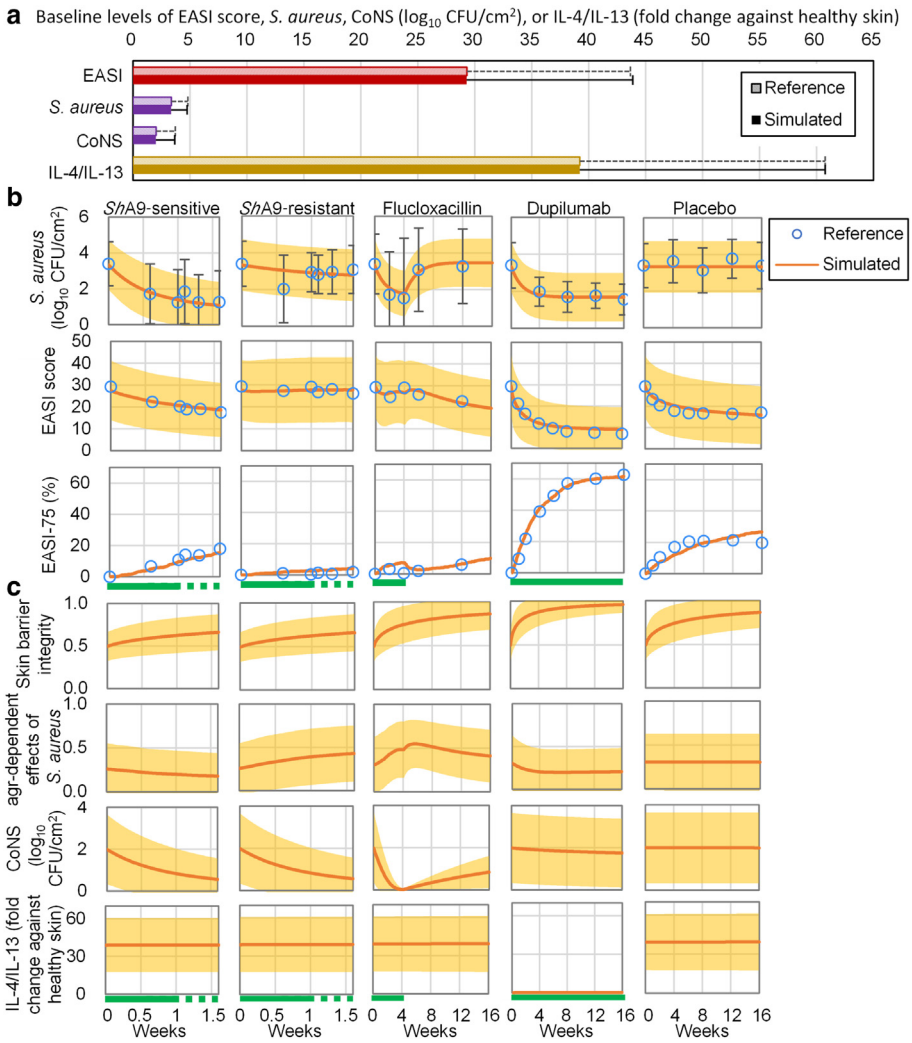

Figure 3. QSP model–based simulation reproduced the reference data. The distributions of the model parameters were optimized to minimize the difference between simulated and reference data ("Optimizing model parameters to reproduce clinical data" in Supplementary Materials and Methods). The simulation was conducted on 1,000 virtual patients. (**a**) Comparison of baseline levels of biological factors between reference (striped bars) and simulated (filled bars) data. Error bars indicate SD. (**b**) Comparison of clinical efficacies of flucloxacillin, *Sh*A9, and dupilumab between reference (unfilled circles denote the mean, error bars indicate SD) and simulated (lines denote the mean, shaded area denotes SD) data. (**c**) Simulated model variables that have no reference data (lines denote the mean, shaded area denotes SD.). The IL-4/IL-13 levels in dupilumab reflect the 99% inhibition of IL-4/IL-13 by dupilumab. Green lines represent dosing periods. Effects of *Sh*A9 were applied in both dosing and follow-up periods in the simulation because the measured amounts of *Sh*A9 on the skin remained higher than the baseline levels during the follow-up periods in the actual clinical trial (Nakatsuji et al., 2021a), whereas the effects of flucloxacillin and dupilumab were applied only during dosing periods. agr, accessory gene regulatory; CFU, colony-forming unit; CoNS, coagulase-negative *Staphylococcus*; EASI, Eczema Area and Severity Index; QSP, quantitative systems pharmacology; *Sh*A9, *Staphyloccocus hominis* A9.

dupilumab, which was further improved (91.9%) by adding 90% inhibition of agr expression.

S. aureus–targeted therapies achieved significant responses in virtual dupilumab poor responders

We also simulated EASI-75 of *S. aureus*–targeted therapies in dupilumab poor responders (Figure 5c). Similar to the results shown earlier for all virtual patients (Figure 5b), lower *S. aureus* levels, higher CoNS levels, and higher inhibition of agr expression showed a better EASI-75 in virtual dupilumab poor responders. The hypothetical *S. aureus*–specific eradication achieved a significant EASI-75 in virtual dupilumab poor responders (42% for *S. aureus*–specific eradication and 61.1% for that with 90% inhibition of agr expression), which were potentiated by simultaneous application of dupilumab (61.5% for *S. aureus*–specific eradication and 79.6% for that with 90% inhibition of agr expression).

DISCUSSION

QSP model–based meta-analysis reveals the mechanism of conflicting efficacies of *S. aureus*–targeted therapies

We developed a QSP model that describes the interactions between *S. aureus* and CoNS in AD pathogenesis (Figure 2) by integrating data and knowledge from published experiments using human samples ("Model structure" in Supplementary Materials and Methods). The model reproduced published data of clinical efficacy for flucloxacillin, *Sh*A9, and dupilumab (Figure 1) regarding the EASI scores, EASI-75, and *S. aureus* levels (Figure 3).

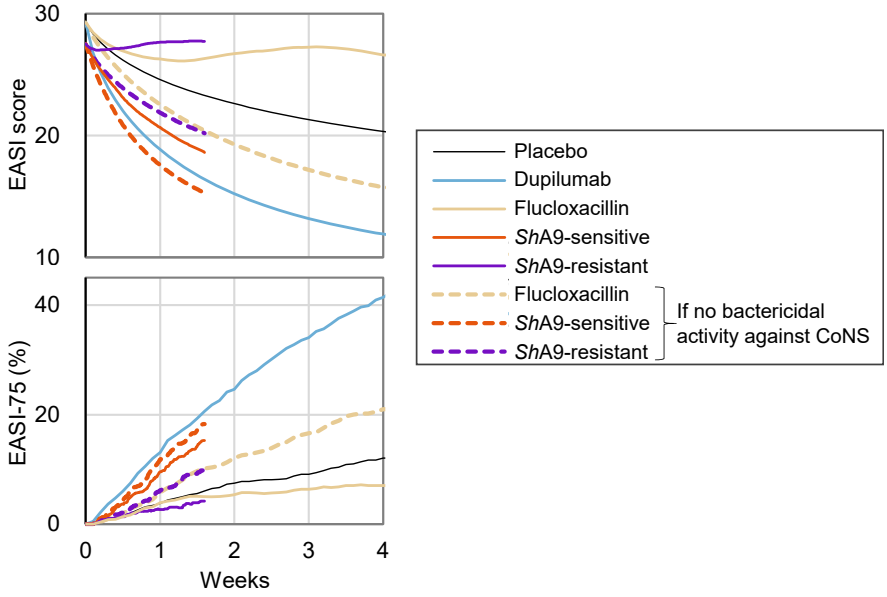

Figure 4. Detrimental effects of flucloxacillin and *Sh*A9 on EASI scores disappeared if their bactericidal activity against CoNS were hypothetically removed. The EASI scores and EASI-75 of flucloxacillin and *Sh*A9 (yellow, red, and purple solid lines) were compared with a hypothetical situation where flucloxacillin and *Sh*A9 have no bactericidal effects on CoNS (yellow-, red-, and purple-dashed lines). The efficacies of dupilumab (blue solid line), the effects of which were modeled by inhibiting IL-4/IL-13 by 99%, were shown as a reference. The simulation was conducted on 1,000 virtual patients (the EASI scores: shown as mean values, EASI-75 denotes the responder rates). Without bactericidal effects on CoNS, flucloxacillin and *Sh*A9 achieved better efficacies than placebo (black thin line) in our simulation. The simulation of efficacies of *Sh*A9 was stopped on day 10 because our model was calibrated to reproduce the reported efficacies of *Sh*A9 until day 10. CoNS, coagulase-negative *Staphylococcus*; EASI, Eczema Area and Severity Index; *Sh*A9, *Staphyloccocus hominis* A9.

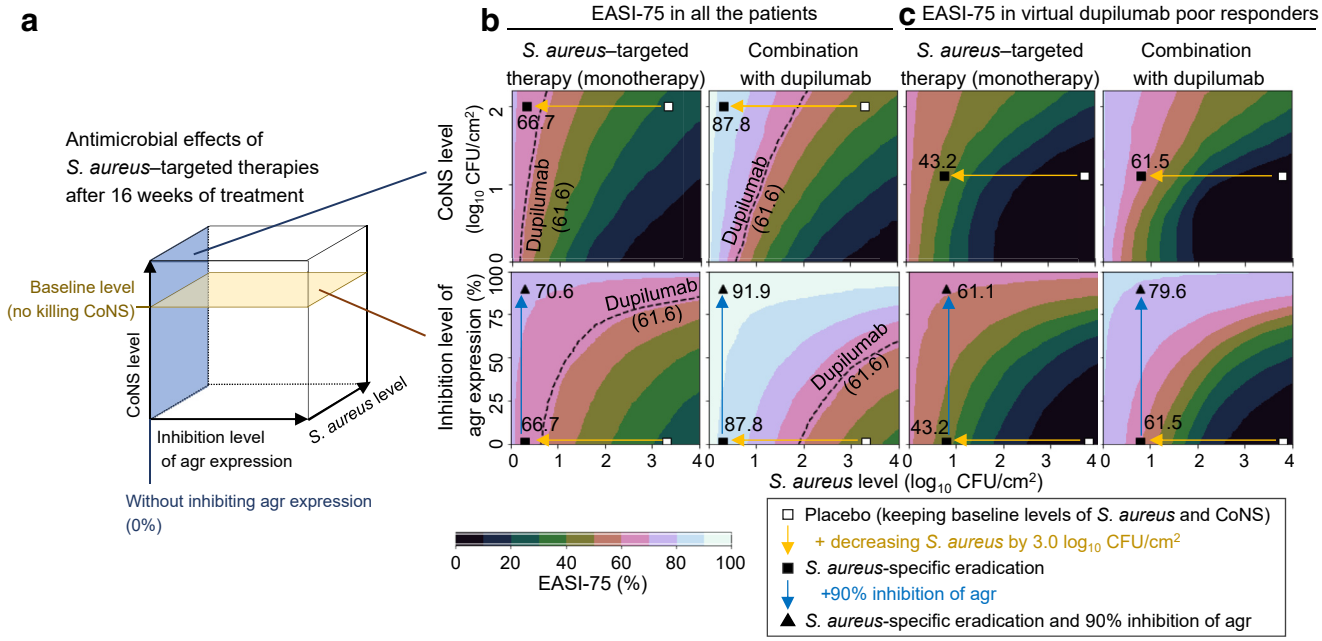

Figure 5. Hypothetical *Staphylococcus aureus*–targeted therapies achieved better EASI-75 after 16 weeks of treatment than dupilumab in our model simulation. (**a**) Antimicrobial effects of hypothetical *S. aureus*–targeted therapies are represented by the level of *S. aureus*, the level of CoNS, and the inhibition level of agr expression after 16 weeks of treatment. Hypothetical *S. aureus*–targeted therapies were represented in our model by varying the strengths of *S. aureus* killing, CoNS killing, and inhibition of agr expression. (**b, c**) Antimicrobial effects of hypothetical *S. aureus*–targeted therapies evaluated by EASI-75 after 16 weeks of treatment (**b**) for all virtual patients and (**c**) for virtual dupilumab poor responders. Lower *S. aureus* levels, higher CoNS levels, and stronger inhibition of agr expression achieved a better EASI-75. The hypothetical *S. aureus*–specific eradication (yellow arrows) achieved (**b**) comparable or (**c**) better EASI-75 than dupilumab (dotted line in **b** and 0% in **c**), and its EASI-75 was potentiated (triangle) by adding 90% inhibition of agr expression (blue arrows). Their combination application with dupilumab achieved better EASI-75 than an application of either alone. The effects of dupilumab were modeled by inhibiting IL-4/IL-13 by 99%. The simulation was conducted on 1,000 virtual patients or 1,000 virtual dupilumab poor responders (levels of *S. aureus* and CoNS and the inhibition level of agr expression: shown as the mean values, EASI-75 denotes the responder rates). agr, accessory gene regulatory; CFU, colony-forming unit; CoNS, coagulase-negative *Staphylococcus*; EASI, Eczema Area and Severity Index.

The QSP model simulation revealed that *S. aureus*–targeted therapies can worsen the EASI scores if they kill CoNS. The simulation showed that the application of *Sh*A9 and flucloxacillin had detrimental effects on AD severity, and those effects disappeared if their bactericidal activity against CoNS was hypothetically removed (Figure 4). A schematic of the QSP model (Figure 2) can explain how a decrease in CoNS impairs the EASI scores. The decreased CoNS levels diminish secreted AIPs, thereby upregulating the agr expression. The upregulated agr expression promotes the production of virulence factors that damage the skin barrier (e.g., by phenol-soluble modulin-α and enterotoxins) and induce inflammation (e.g., by wall teichoic acid to activate dendritic cells), which can worsen AD severity. These results and interpretation indicate the importance of bactericidal specificity on *S. aureus* in *S. aureus*–targeted therapies.

Model simulation quantifies the relationships between profiles of antibacterial effects and responder rates

The QSP model simulation enables a quantitative discussion on the clinical efficacies of hypothetical therapies, which cannot be achieved using only qualitative models (Figure 2).

Our simulation elucidated the quantitative relationships between antibacterial effects of *S. aureus*–targeted therapies (decreases in the *S. aureus* and CoNS levels and in the agr expression level) and their EASI-75 responder rates (Figure 5b, left). In addition, our simulation suggested that the efficacy of *S. aureus*–targeted therapies can be potentiated by concomitant use of dupilumab (Figure 5b, right).

Theoretically, *S. aureus*–targeted therapies will achieve the best efficacy if they eradicated *S. aureus* completely. However, some *S. aureus* may remain on population average after *S. aureus*–targeted therapies presumably because of resistance to antibiotics and bacteriocins (Harkins et al., 2019). Hence, it is crucial to inhibit agr expression by keeping the AIPs produced by CoNS, in addition to killing *S. aureus,* to minimize the agr-dependent virulence effects of *S. aureus*.

Hypothetical *S. aureus*–specific eradication (the maximal reduction of *S. aureus* level without killing CoNS), especially in combination with dupilumab, showed higher responder rates than dupilumab alone (simulated EASI-75 on week 16: 26.6% for placebo, 61.6% for dupilumab, 66.7% for *S. aureus*–specific eradication, and 87.8% for combination) (Figure 5b, right). Recently, Jak inhibitors have shown promising efficacies in patients with AD; abrocitinib showed a response comparable with that of dupilumab (EASI-75 on week 16: 71.0% for abrocitinib vs. 65.5% for dupilumab, not significant) (Bieber et al., 2021), and upadacitinib showed the highest responder rate among phase 3 trials of Jak inhibitors (EASI-75 on week 16. 77.1% for upadacitinib vs. 26.4% for placebo) (Reich et al., 2021). Our simulation implies that *S. aureus*–specific eradication, combined with dupilumab, may achieve higher responder rates than Jak inhibitors. This quantitative comparison of clinical efficacies between hypothetical and existing therapies is one of the benefits of model simulation.

***S. aureus*–specific eradication is potentially effective for dupilumab poor responders**

Another benefit of model simulation is that it can compute the expected clinical efficacies of hypothetical therapies in specific subpopulations. This study also suggested the effectiveness of *S. aureus*–specific eradication for dupilumab poor responders. Simulation for virtual dupilumab poor responders showed that *S. aureus*–specific eradication achieved 43.2% EASI-75 (Figure 5c, left), which is much higher than the EASI-75 achieved (up to 33.8%) when we simulated the inhibition of all the cytokines considered in the previous QSP model of biologics (Miyano et al., 2021). These results imply that *S. aureus* rather than cytokines is potentially a promising therapeutic target for dupilumab poor responders.

The model simulation also showed that the efficacy of *S. aureus*–targeted therapies is potentiated by its concomitant use with dupilumab in dupilumab poor responders (Figure 5c, right). The results suggest that IL-4/IL-13 signaling contributes to the pathogenesis even for dupilumab poor responders and thus needs to be inhibited. Targeting both *S. aureus* and IL-4/IL-13 could be a promising therapeutic approach for patients with AD.

Limitation of the QSP model simulation

This study aimed to interpret published clinical data on *S. aureus*–targeted therapies obtained under different study conditions using a model-based meta-analysis. We assumed that their efficacies are comparable across clinical trials after normalization, although the study conditions (e.g., topical and systemic therapies) may influence the reported efficacies. For example, one of the clinical trials (Nakatsuji et al., 2021a) evaluated the efficacies of *Sh*A9 for a short period (10 days), posing uncertainty on its long-term efficacy. The accuracy of the simulated efficacies of the hypothetical *S. aureus*–targeted therapies needs to be verified by future clinical trials (Cucurull-Sanchez et al., 2019).

We made our model as simple as possible to concisely interpret the clinical efficacies of *S. aureus*–targeted therapies with reference to AD pathogenesis. There are several factors that our model omitted because they were not relevant in this study. For example, our model approximates pharmacokinetics as a switch-like behavior (treatment effects are switched on at the start of dosing and are switched off at the end of dosing). Modeling of AD pathogenesis considered the cutaneous compartment of skin lesions (e.g., without considering cytokines in the blood), excluded the potential roles of other microbes than *S. aureus* and CoNS, does not explicitly describe some biological factors such as AMPs and immune cells, and simplified some pathways (e.g., IL-4 and IL-13 increase *S. aureus* and CoNS by decreasing AMPs, where AMPs were not described as a model variable). Our model could be further expanded when those omitted factors become relevant for a specific investigation.

Our model assumed that CoNS has no detrimental effects on the skin barrier and inflammation. However, recent studies have suggested that *S. epidermidis*, one of CoNS, also has detrimental effects on skin barrier (Cau et al., 2021). The detrimental effects of *S. epidermidis* may explain the worsened EASI scores in *Sh*A9 because it increased the proportion of *S. epidermidis* among microbiome in the AD skin lesion (Nakatsuji et al., 2021a). Explicit modeling of different CoNS strains may deliver further insights into the roles of CoNS in AD pathogenesis, although our model assumed that the detrimental effects of *S. epidermidis* are negligible compared

Table 1. Treatments Considered in this Study

Treatments	Targets	Dose Regimen (Highest Dose)	Reported Efficacies	No. of Patients in Placebo/ Treatment Group (Phase)
*Sh*A9 (Nakatsuji et al., 2021a)	Microbes	2 g (to deliver 1 × 10^6 CFU/cm^2) twice/day, topical, for 1 week (follow-up until 10 days)	Percentage-improved local EASI[1] *S. aureus*	17/35 (phase 1). Of 35 patients, 21 and 11 patients were colonized with *S. aureus* that is sensitive and resistant to *Sh*A9 bacteriocin, respectively. The colonization status of the remaining three patients was not determined
Flucloxacillin (Ewing et al., 1998)	Microbes	250 mg for four times/day, oral, for 4 weeks (follow-up until 12 weeks)	Surface area score[2] Erythema score[2] *S. aureus*	25/25 (phase 2)
Dupilumab (anti–IL-4 receptor subunit α antibody) (Callewaert et al., 2020; Blauvelt et al., 2017; Guttman-Yassky et al., 2019a)	IL-4 and IL-13	400 mg followed by 200 mg weekly, subcutaneous	EASI-75 Percentage-improved EASI *S. aureus*	27/27 (phase 2)
		600 mg followed by 300 mg, weekly, subcutaneous, with concomitant use of topical corticosteroids	EASI-75, Percentage-improved EASI	264/270 (phase 3)

Abbreviations: CFU, colony-forming unit; EASI, Eczema Area and Severity Index; No., number; ShA9, *Staphyloccocus hominis* A9.
[1]We used percentage-improved local EASI for percentage-improved EASI because *Sh*A9 was applied on the ventral forearms locally.
[2]We regarded percentage-improved score of a product of the surface area score and the erythema score as the percentage-improved EASI by assuming that the erythema represents the four signs (erythema, induration, excoriations, and lichenification) for the EASI score, which is calculated as a product of the area score and the severity score of the four signs. For dupilumab, we adopted *S. aureus* levels in phase 2 study and the percentage-improved EASI and EASI-75 in phase 3 study ("Selection of clinical studies for development of the quantitative systems pharmacology model" in Supplementary Materials and Methods).

with those of *S. aureus* because *S. aureus* has a higher correlation with AD severity scores than *S. epidermidis* (Byrd et al., 2017; Ederveen et al., 2019).

Prospect for *S. aureus*–targeted therapies

The results of this study support the widely accepted idea that *S. aureus* is a promising drug target for AD and suggests the potential importance of considering antibacterial activities against both *S. aureus* and CoNS when developing *S. aureus*–targeted therapies. How much *S. aureus* killing is required to achieve a set efficacy for any given therapy would depend on how strongly the therapy kills CoNS and inhibits agr expression.

This study presents an example of how QSP model can contribute to model-informed drug development (EFPIA MID3 Workgroup et al., 2016) for precision medicine. For example, our simulation results will contribute to the design of *S. aureus*–targeted therapies because the simulated relationship between EASI-75 responder rates and antibacterial effects (i.e., decreases in the *S. aureus* and CoNS levels and inhibition of agr expression) can be used as a guide to set a target profile of the antibacterial effects to achieve a desirable efficacy (e.g., better EASI-75 than dupilumab). Our simulation results also encourage a combinatorial use of *S. aureus*–targeted therapies and cytokine-targeted therapies such as biologics and Jak inhibitors for AD.

MATERIALS AND METHODS

Our QSP model explicitly describes the causal relationships between treatments, biological factors, and an AD severity score using a graphical scheme and ordinary differential equations. The model was developed by (i) selecting treatments and biological factors to be modeled, (ii) formulating treatment effects and causal relationships between the biological factors, and (iii) optimizing model parameters that define virtual patients. The developed model was used to simulate the clinical efficacies of hypothetical *S. aureus*–targeted therapies in virtual patients.

Selecting treatments and biological factors

We considered flucloxacillin, *Sh*A9, and dupilumab because they showed a decrease in *S. aureus* levels in a placebo-controlled double-blinded clinical study, where AD severity scores were reported (Table 1 and "Selection of clinical studies for development of the quantitative systems pharmacology model" in Supplementary Materials and Methods).

We selected six biological factors as model variables: colony density levels of *S. aureus* and CoNS and levels of agr expression, IL-4/IL-13 in the skin, skin barrier integrity, and the EASI score (Supplementary Table S2). *S. aureus* and CoNS are the core factors in this study. CoNS does not include the *Sh*A9 strain applied in the *Sh*A9 treatment. Agr expression corresponds to the main mechanism for *S. aureus* to express virulence factors in *S. aureus* (Williams et al., 2019) that induce skin barrier damage and skin inflammation. The IL-4/IL-13 represents T helper 2 cytokines that are targeted by dupilumab. Skin barrier integrity is a critical factor in AD pathogenesis, as in our previous models (Miyano et al., 2021; Domínguez-Hüttinger et al., 2017). The EASI score represents an endpoint for AD severity. Some biological factors such as AMPs were not described as model variables but were considered implicitly as a rationale for the causal relationships (e.g., IL-4 and IL-13 increase *S. aureus* and CoNS by decreasing AMPs) to make the model simpler yet interpretable.

Formulating treatment effects and causal relationships between biological factors

We developed a mathematical model consisting of six equations, corresponding to the six biological factors with 26 parameters to simulate the efficacies of the three treatments ("Model structure" in

Supplementary Materials and Methods). The effects of flucloxacillin were modeled by increasing the killing rates of both *S. aureus* and CoNS because its antibacterial spectrum covers all *Staphylococcus* species. The effects of *Sh*A9 were modeled by increasing the killing rates of *S. aureus* and CoNS and the inhibitory strength against the agr expression because *Sh*A9 produces bacteriocins against both *S. aureus* and CoNS (Nakatsuji et al., 2017) and AIPs that inhibit the agr expression (Nakatsuji et al., 2021a). The effects of dupilumab were modeled by decreasing the effective concentrations of IL-4/IL-13 in the skin by 99%. The value of 99% was obtained from a calculation using the published data on half-maximal inhibitory concentration and the mean concentration of drugs in the skin (Vazquez et al., 2018) that was estimated from their concentration in the serum measured in clinical trials ("Treatment effects" in Supplementary Materials and Methods). The causal relationships between biological factors were described according to published experimental evidence on the basis of human data ("Biological factors" in Supplementary Materials and Methods). The model was implemented in Python 3.7.6 (Python Software Foundation, Fredericksburg, VA).

Modeling virtual patients and optimizing model parameters

We assumed that the model parameter values (e.g., the recovery rate of skin barrier through skin turnover, k_1) vary between patients with AD and that a set of 26 parameter values defines the pathophysiological backgrounds of each virtual patient (Supplementary Table S3). Each value of the i-th parameter, k_i, is taken from a log-normal distribution (Limpert et al., 2001) whose probability function, $f(k_i)$, is defined by

$$f(k_i) = \frac{1}{\sqrt{2\pi}\sigma_i k_i} \exp\left(-\frac{(\ln k_i - \mu_i)^2}{2\sigma_i^2} \right), \quad (1)$$

where μ_i and σ_i are the distribution parameters that represent the mean and the SD of $\ln k_i$, respectively.

We optimized the 52 distribution parameters (μ_i and σ_i, $i = 1, \ldots, 26$) that define the distributions of the 26 model parameters so that the model minimizes the root mean square errors of both mean values and SDs between simulated data and the reference data derived from published clinical studies ("Optimizing model parameters to reproduce clinical data" in Supplementary Materials and Methods). The reference data consist of baseline levels of *S. aureus*, CoNS, IL-4/IL-13, and the EASI scores (Supplementary Table S2) and time courses of *S. aureus* levels, EASI scores, and EASI-75 assessed in clinical trials of the selected treatments (Figure 1). The *S. aureus* levels, EASI scores, and EASI-75 were normalized to compare the clinical efficacies of different clinical trials ("Data processing" in Supplementary Materials and Methods). agr expression and skin barrier integrity were regarded as latent state variables that have no reference data to be compared with simulated values. Simulated baseline levels were obtained by computing steady-state levels of biological factors (at 1,000 weeks without treatment). All the simulations were conducted on 1,000 virtual patients, generated by randomly sampling each parameter value from the distribution in equation (1).

Simulating efficacies of hypothetical *S. aureus*–targeted therapies

We simulated EASI-75 of hypothetical therapies with different strengths for the killing of *S. aureus* and CoNS and for inhibiting agr expression to explore optimal *S. aureus*–targeted therapies. Specifically, we examined the efficacies of hypothetical therapies that achieve a maximal reduction in *S. aureus* level from placebo (a reduction of 3.0 $\log_{10}$ colony-forming unit per cm^2; the reported maximal reduction is 3.1 $\log_{10}$ colony-forming unit per cm^2 by cefuroxime axetil [Boguniewicz et al., 2001] and neomycin [Leyden and Kligman, 1977] among published clinical trials for *S. aureus*–targeted therapies [Boguniewicz et al., 2001; Breneman et al., 2000; Ewing et al., 1998; Hung et al., 2007; Korting et al., 1994; Leyden and Kligman, 1977; Nakatsuji et al., 2021a]), the maximal level of CoNS (no bactericidal effects on CoNS, keeping the baseline level of CoNS), an exemplary level of inhibition of the agr expression (we used 90% because we have no reliable evidence to estimate the maximal inhibition rates of agr expression), and their combinations.

We also simulated EASI-75 of hypothetical therapies in virtual dupilumab poor responders, which were defined as the virtual patients who did not achieve the EASI-75 criterion at 16 weeks.

Data availability statement

The code of the QSP model is available at https://github.com/Tanaka-Group/AD_QSP_model.

ORCIDs

Takuya Miyano: http://orcid.org/0000-0002-1181-6924
Alan D. Irvine: http://orcid.org/0000-0002-9048-2044
Reiko J. Tanaka: http://orcid.org/0000-0002-0769-9382

AUTHOR CONTRIBUTIONS

Conceptualization: TM, RJT; Data Curation: TM; Formal Analysis: TM; Funding Acquisition: RJT; Investigation: TM; Methodology: TM; Project Administration: RJT; Resources: RJT; Software: TM; Supervision: RJT; Validation: TM; Visualization: TM; Writing — Original Draft Preparation: TM, RJT; Writing — Review and Editing: TM, ADI, RJT

ACKNOWLEDGMENTS

We thank Elisa Domínguez-Hüttinger for her insightful comments on our manuscript. This work was funded by the British Skin Foundation (005/R/18).

CONFLICT OF INTEREST

TM reports personal fees from DAIICHI SANKYO during the conduct of this study, outside the submitted work; ADI reports personal fees from Sanofi Regeneron, AbbVie, Eli Lilly, Pfizer, UCB Pharma, Novartis, Dermavant, Benevolent AI, Menlo Therapeutics, Chugai, LEO Pharma, and Arena during the conduct of this study, all outside the submitted work; and RJT reports grants from British Skin Foundation during the conduct of the study.

SUPPLEMENTARY MATERIAL

Supplementary material is linked to the online version of the paper at www.jidonline.org, and at https://doi.org/10.1016/j.xjidi.2022.100110.

REFERENCES

Alexander H, Paller AS, Traidl-Hoffmann C, Beck LA, De Benedetto A, Dhar S, et al. The role of bacterial skin infections in atopic dermatitis: expert statement and review from the International Eczema Council Skin Infection Group. Br J Dermatol 2020;182:1331–42.

Bieber T, Simpson EL, Silverberg JI, Thaçi D, Paul C, Pink AE, et al. Abrocitinib versus placebo or dupilumab for atopic dermatitis. N Engl J Med 2021;384:1101–12.

Blauvelt A, de Bruin-Weller M, Gooderham M, Cather JC, Weisman J, Pariser D, et al. Long-term management of moderate-to-severe atopic dermatitis with dupilumab and concomitant topical corticosteroids (LIBERTY AD CHRONOS): a 1-year, randomised, double-blinded, placebo-controlled, phase 3 trial. Lancet 2017;389:2287–303.

Boguniewicz M, Sampson H, Leung SB, Harbeck R, Leung DY. Effects of cefuroxime axetil on Staphylococcus aureus colonization and superantigen production in atopic dermatitis. J Allergy Clin Immunol 2001;108:651–2.

Breneman DL, Hanifin JM, Berge CA, Keswick BH, Neumann PB. The effect of antibacterial soap with 1.5% triclocarban on Staphylococcus aureus in patients with atopic dermatitis. Cutis 2000;66:296–300.

Breuer K, HAussler S, Kapp A, Werfel T. Staphylococcus aureus: colonizing features and influence of an antibacterial treatment in adults with atopic dermatitis. Br J Dermatol 2002;147:55–61.

Byrd AL, Deming C, Cassidy SKB, Harrison OJ, Ng WI, Conlan S, et al. *Staphylococcus aureus* and *Staphylococcus epidermidis* strain diversity underlying pediatric atopic dermatitis. Sci Transl Med 2017;9: eaal4651.

Callewaert C, Nakatsuji T, Knight R, Kosciolek T, Vrbanac A, Kotol P, et al. IL-4Rα blockade by dupilumab decreases Staphylococcus aureus colonization and increases microbial diversity in atopic dermatitis. J Invest Dermatol 2020;140:191–202.e7.

Cau L, Williams MR, Butcher AM, Nakatsuji T, Kavanaugh JS, Cheng JY, et al. Staphylococcus epidermidis protease EcpA can be a deleterious component of the skin microbiome in atopic dermatitis. J Allergy Clin Immunol 2021;147:955–66.e16.

Clowry J, Irvine AD, McLoughlin RM. Next-generation anti-Staphylococcus aureus vaccines: a potential new therapeutic option for atopic dermatitis? J Allergy Clin Immunol 2019;143:78–81.

Cucurull-Sanchez L, Chappell MJ, Chelliah V, Amy Cheung SY, Derks G, Penney M, et al. Best practices to maximize the use and reuse of quantitative and systems pharmacology models: recommendations from the United Kingdom quantitative and systems pharmacology network. CPT Pharmacometrics Syst Pharmacol 2019;8:259–72.

Czarnowicki T, He H, Krueger JG, Guttman-Yassky E. Atopic dermatitis endotypes and implications for targeted therapeutics. J Allergy Clin Immunol 2019;143:1–11.

Deckers IA, McLean S, Linssen S, Mommers M, van Schayck CP, Sheikh A. Investigating international time trends in the incidence and prevalence of atopic eczema 1990–2010: a systematic review of epidemiological studies. PLoS One 2012;7:e39803.

Domínguez-Hüttinger E, Christodoulides P, Miyauchi K, Irvine AD, Okada-Hatakeyama M, Kubo M, et al. Mathematical modeling of atopic dermatitis reveals "double-switch" mechanisms underlying 4 common disease phenotypes. J Allergy Clin Immunol 2017;139:1861–72.e7.

Ederveen THA, Smits JPH, Hajo K, et al. A generic workflow for single locus sequence typing (SLST) design and subspecies characterization of microbiota. Sci Rep 2019;9:19834.

EFPIA MID3 Workgroup, Marshall SF, Burghaus R, Cosson V, Cheung SY, Chenel M, et al. Good practices in model-informed drug discovery and development: practice, application, and documentation. CPT Pharmacometrics Syst Pharmacol 2016;5:93–122.

Elias PM. The how, why and clinical importance of stratum corneum acidification. Exp Dermatol 2017;26:999–1003.

Ewing CI, Ashcroft C, Gibbs AC, Jones GA, Connor PJ, David TJ. Flucloxacillin in the treatment of atopic dermatitis. Br J Dermatol 1998;138: 1022–9.

Geoghegan JA, Irvine AD, Foster TJ. Staphylococcus aureus and atopic dermatitis: a complex and evolving relationship. Trends Microbiol 2018;26:484–97.

George SM, Karanovic S, Harrison DA, Rani A, Birnie AJ, Bath-Hextall FJ, et al. Interventions to reduce Staphylococcus aureus in the management of eczema. Cochrane Database Syst Rev 2019;2019:CD003871.

Gibbs JP, Menon R, Kasichayanula S. Bedside to bench: integrating quantitative clinical pharmacology and reverse translation to optimize drug development. Clin Pharmacol Ther 2018;103:196–8.

Gong JQ, Lin L, Lin T, Hao F, Zeng FQ, Bi ZG, et al. Skin colonization by Staphylococcus aureus in patients with eczema and atopic dermatitis and relevant combined topical therapy: a double-blind multicentre randomized controlled trial. Br J Dermatol 2006;155:680–7.

Guttman-Yassky E, Bissonnette R, Ungar B, Suárez-Fariñas M, Ardeleanu M, Esaki H, et al. Dupilumab progressively improves systemic and cutaneous abnormalities in patients with atopic dermatitis. J Allergy Clin Immunol 2019a;143:155–72.

Guttman-Yassky E, Pavel AB, Zhou L, Estrada YD, Zhang N, Xu H, et al. GBR 830, an anti-OX40, improves skin gene signatures and clinical scores in patients with atopic dermatitis. J Allergy Clin Immunol 2019b;144: 482–93.e7.

Hanifin JM, Thurston M, Omoto M, Cherill R, Tofte SJ, Graeber M. The eczema area and severity index (EASI): assessment of reliability in atopic dermatitis. EASI Evaluator Group. Exp Dermatol 2001;10:11–8.

Harkins CP, Holden MTG, Irvine AD. Antimicrobial resistance in atopic dermatitis: need for an urgent rethink. Ann Allergy Asthma Immunol 2019;122:236–40.

Hendricks AJ, Lio PA, Shi VY. Management recommendations for dupilumab partial and non-durable responders in atopic dermatitis. Am J Clin Dermatol 2019;20:565–9.

Higaki S, Morohashi M, Yamagishi T, Hasegawa Y. Comparative study of staphylococci from the skin of atopic dermatitis patients and from healthy subjects. Int J Dermatol 1999;38:265–9.

Howell MD, Boguniewicz M, Pastore S, Novak N, Bieber T, Girolomoni G, et al. Mechanism of HBD-3 deficiency in atopic dermatitis. Clin Immunol 2006;121:332–8.

Howell MD, Kim BE, Gao P, Grant AV, Boguniewicz M, DeBenedetto A, et al. Cytokine modulation of atopic dermatitis filaggrin skin expression. J Allergy Clin Immunol 2009;124(3 Suppl. 2):R7–12.

Hung SH, Lin YT, Chu CY, Lee CC, Liang TC, Yang YH, et al. Staphylococcus colonization in atopic dermatitis treated with fluticasone or tacrolimus with or without antibiotics. Ann Allergy Asthma Immunol 2007;98:51–6.

Katsuyama M, Kobayashi Y, Ichikawa H, Mizuno A, Miyachi Y, Matsunaga K, et al. A novel method to control the balance of skin microflora part 2. A study to assess the effect of a cream containing farnesol and xylitol on atopic dry skin [published correction appears in J Dermatol Sci 2005;39: 197]. J Dermatol Sci 2005;38:207–13.

Korting HC, Zienicke H, Braun-Falco O, Bork K, Milbradt R, Nolting S, et al. Modern topical glucocorticoids and anti-infectives for superinfected atopic eczema: do prednicarbate and didecyldimethylammoniumchloride form a rational combination [published correction appears in Infection 1995;23: 67]? Infection 1994;22:390–4.

Lambers H, Piessens S, Bloem A, Pronk H, Finkel P. Natural skin surface pH is on average below 5, which is beneficial for its resident flora. Int J Cosmet Sci 2006;28:359–70.

Langan SM, Irvine AD, Weidinger S. Atopic dermatitis [published correction appears in Lancet 2020;396:758]. Lancet 2020;396:345–60.

LePoidevin LM, Lee DE, Shi VY. A comparison of international management guidelines for atopic dermatitis. Pediatr Dermatol 2019;36:36–65.

Leyden JJ, Kligman AM. The case for steroid–antibiotic combinations. Br J Dermatol 1977;96:179–87.

Limpert E, Stahel WA, Abbt M. Log-normal distributions across the sciences: keys and clues: on the charms of statistics, and how mechanical models resembling gambling machines offer a link to a handy way to characterize log-normal distributions, which can provide deeper insight into variability and probability-normal or log-normal: that is the question. BioScience 2001;51:341–52.

Miyano T, Irvine AD, Tanaka RJ. A mathematical model to identify optimal combinations of drug targets for dupilumab poor responders in atopic dermatitis. Allergy 2021;77:582–94.

Nakatsuji T, Chen TH, Narala S, Chun KA, Two AM, Yun T, et al. Antimicrobials from human skin commensal bacteria protect against Staphylococcus aureus and are deficient in atopic dermatitis. Sci Transl Med 2017;9:eaah4680.

Nakatsuji T, Gallo RL, Shafiq F, Tong Y, Chun K, Butcher AM, et al. Use of autologous bacteriotherapy to treat *Staphylococcus aureus* in patients with atopic dermatitis: A randomized double-blind clinical trial. JAMA Dermatol 2021b;157:978–82.

Nakatsuji T, Hata TR, Tong Y, Cheng JY, Shafiq F, Butcher AM, et al. Development of a human skin commensal microbe for bacteriotherapy of atopic dermatitis and use in a phase 1 randomized clinical trial. Nat Med 2021a;27:700–9.

Nath S, Kumari N, Bandyopadhyay D, Sinha N, Majumder PP, Mitra R, et al. Dysbiotic lesional microbiome with filaggrin missense variants associate with atopic dermatitis in India. Front Cell Infect Microbiol 2020;10: 570423.

Park HY, Kim CR, Huh IS, Jung MY, Seo EY, Park JH, et al. Staphylococcus aureus colonization in acute and chronic skin lesions of patients with atopic dermatitis. Ann Dermatol 2013;25:410–6.

Reich K, Teixeira HD, de Bruin-Weller M, Bieber T, Soong W, Kabashima K, et al. Safety and efficacy of upadacitinib in combination with topical corticosteroids in adolescents and adults with moderate-to-severe atopic dermatitis (AD Up): results from a randomised, double-blind, placebo-

controlled, phase 3 trial [published corrections appear in Lancet 2021;397: 2336 and Lancet 2021;398:746]. Lancet 2021;397:2169–81.

Schoeberl B. Quantitative systems pharmacology models as a key to translational medicine. Curr Opin Syst Biol 2019;16:25–31.

Schram ME, Spuls PI, Leeflang MMG, Lindeboom R, Bos JD, Schmitt J, et al. EASI, (objective) SCORAD and POEM for atopic eczema: responsiveness and minimal clinically important difference. Allergy 2012;67:99–106.

Seltmann J, Roesner LM, von Hesler FW, Wittmann M, Werfel T. IL-33 impacts on the skin barrier by downregulating the expression of filaggrin. J Allergy Clin Immunol 2015;135:1659–61.e4.

Simpson EL, Bieber T, Eckert L, Wu R, Ardeleanu M, Graham NM, et al. Patient burden of moderate to severe atopic dermatitis (AD): insights from a phase 2b clinical trial of dupilumab in adults. J Am Acad Dermatol 2016a;74:491–8.

Simpson EL, Bieber T, Guttman-Yassky E, Beck LA, Blauvelt A, Cork MJ, et al. Two phase 3 trials of dupilumab versus placebo in atopic dermatitis. N Engl J Med 2016b;375:2335–48.

Syed AK, Reed TJ, Clark KL, Boles BR, Kahlenberg JM. Staphlyococcus aureus phenol-soluble modulins stimulate the release of proinflammatory cytokines from keratinocytes and are required for induction of skin inflammation [published correction appears in Infect Immun 2015;83: 4450]. Infect Immun 2015;83:3428–37.

Tham EH, Koh E, Common JEA, Hwang IY. Biotherapeutic approaches in atopic dermatitis. Biotechnol J 2020;15:e1900322.

Vazquez ML, Kaila N, Strohbach JW, Trzupek JD, Brown MF, Flanagan ME, et al. Identification of N-{cis-3-[methyl(7H-pyrrolo[2,3-d]pyrimidin-4-yl) amino]cyclobutyl}propane-1-sulfonamide (PF-04965842): a selective JAK1 clinical candidate for the treatment of autoimmune diseases. J Med Chem 2018;61:1130–52.

Weidinger S, Beck LA, Bieber T, Kabashima K, Irvine AD. Atopic dermatitis. Nat Rev Dis Primers 2018;4:1.

Williams MR, Costa SK, Zaramela LS, Khalil S, Todd DA, Winter HL, et al. Quorum sensing between bacterial species on the skin protects against epidermal injury in atopic dermatitis. Sci Transl Med 2019;11:eaat8329.

SUPPLEMENTARY MATERIALS AND METHODS

Selection of clinical studies for development of the quantitative systems pharmacology model

We used predefined inclusion and exclusion criteria (Supplementary Figure S1) to select clinical studies to be referenced in the development of the quantitative systems pharmacology model. First, we identified 24 clinical trials that reported both *Staphyloccocus aureus* levels and atopic dermatitis (AD) severity scores in a placebo-controlled study. We then excluded 18 clinical trials because the treatments have unclear mechanisms of action, they failed to decrease *S. aureus* levels compared with placebo, or they evaluated only a small number (<10) of patients. Supplementary Table S3 lists the treatments excluded in this study. As for antibiotics/antiseptics, 23 clinical trials were investigated in Cochrane review (George et al., 2019), from which we included only one study (Ewing et al., 1998) with flucloxacillin, which met our inclusion criteria.

As for dupilumab, we included the data of *S. aureus* levels in a phase 2 study (Callewaert et al., 2020) and the percentage-improved Eczema Area and Severity Index (EASI) and EASI-75 in a phase 3 study (Blauvelt et al., 2017). The detailed rationale for this choice is as follows:

1. Percentage-improved EASI and EASI-75 were reported in both phase 2 and phase 3 studies. However, *S. aureus* levels were reported only in the phase 2 study (Callewaert et al., 2020).
2. The measured percentage-improved EASI of placebo treatment in the phase 2 study (Callewaert et al., 2020) is not deemed to be reliable because the relationship between measured percentage-improved EASI scores and EASI-75 on week 16 deviates from those in other clinical trials (Supplementary Figure S2, left).
3. The estimated percentage-improved EASI by mixed-effect model repeated measure, which is a popular method to handling missing data (e.g., owing to drop out of patients during a clinical study) (Lane, 2008), in the phase 2 study (Callewaert et al., 2020) is deemed to be reliable because the relationship between the estimated percentage-improved EASI and EASI-75 on week 16 in the phase 2 study (Callewaert et al., 2020) is consistent with those in other clinical trials (Supplementary Figure S2, left). However, the estimated value is not time-course data (reported week 16 only) and cannot be used for our model fitting.
4. We decided to use a phase 3 study (Blauvelt et al., 2017) that reported time-course data of percentage-improved EASI and EASI-75 because (i) the percentage-improved EASI on week 16 in the phase 3 study (Blauvelt et al., 2017) is comparable with the estimated percentage-improved EASI by mixed-effect model repeated measure on week 16 in the phase 2 study (Callewaert et al., 2020) (Supplementary Figure S2; right, the open and closed circles) and (ii) time-course data of the percentage-improved EASI of dupilumab treatment in phase 2 were comparable with those in phase 3 (Supplementary Figure S2, right; the blue crosses and filled circles), suggesting that time-course data of percentage-improved EASI of placebo treatment in phase 2, if they were estimated by mixed-effect model repeated measure, are comparable with those in phase 3.
5. Among several phase 3 studies for dupilumab (Blauvelt et al., 2017; Simpson et al., 2016), we selected a phase 3 study that used combination therapy with topical corticosteroids (Blauvelt et al., 2017) because the combination therapy is more reflective of the likely clinical use than monotherapy.

Data processing

We used clinical efficacies (*S. aureus* levels, percentage-improved EASI, EASI scores, and EASI-75) of flucloxacillin, *S. hominis* A9 (*Sh*A9), and dupilumab as the reference data. The clinical efficacies were normalized to compare data from different clinical trials.

Normalization of S. aureus levels. Time courses of *S. aureus* levels were reported in clinical trials of flucloxacillin (Ewing et al., 1998), *Sh*A9 (Nakatsuji et al., 2021a), and dupilumab (Callewaert et al., 2020). We described the normalized *S. aureus* level, $a_j(t)$, for the j-th treatment at time t by

$$a_j(t) = \left(\Delta a_j^*(t) - \Delta a_{\mathrm{P}_j}^*(t)\right) + \Delta a_{\mathrm{P}_d}^*(t) + a_{\mathrm{ShA9}}^*(0), \qquad \text{(S1)}$$

where the first term corresponds to the net effects of the treatment defined by the difference of the change in *S. aureus* levels ($\log_{10}$ scale) at time t from baseline, between the j-th treatment ($\Delta a_j^*(t)$) and the corresponding placebo groups ($\Delta a_{\mathrm{P}_j}^*(t)$). This term adjusts for different placebo effects across clinical studies that may differ in the study participants' background, concomitant drugs, and the study sites (Wang et al., 2019). The remaining two terms describe the change in *S. aureus* levels at time t from baseline, $\Delta a_{\mathrm{P}_d}^*(t)$, in the placebo group in the dupilumab clinical trial that evaluated efficacies for the longest period among the trials evaluated in this study and the baseline level of *S. aureus*, $a_{\mathrm{ShA9}}^*(0)$, in the *Sh*A9 clinical trial that is the only one reporting the levels of both *S. aureus* and coagulase-negative *Staphylococcus* (CoNS) among the trials evaluated in this study.

Conversion of reported AD severity scores to percentage-improved EASI, percentage-improved EASI for flucloxacillin, and ShA9. For flucloxacillin, we substituted the percentage-improved EASI for the percentage-improved score of a product of the area score and the severity score of erythema (Ewing et al., 1998) (the only disease sign evaluated in that study) by assuming that the erythema represents the four disease signs (erythema, induration, excoriations, and lichenification) for EASI score, which is calculated as a product of the area score and the severity score of the four signs.

For *Sh*A9, we substituted the percentage-improved EASI for the percentage-improved local EASI of the ventral arms because *Sh*A9 was applied on the ventral forearms locally (Nakatsuji et al., 2021a).

Normalization of the percentage-improved EASI, EASI score, and EASI-75. The percentage-improved EASI, EASI score, and EASI-75 were normalized in the same way as in the published paper on the quantitative systems pharmacology

model of biologics (Miyano et al., 2021). We described normalized percentage-improved EASI, $m_j(t)$, for the j-th treatment at t by the following:

$$m_j(t) = \left(m_j^*(t) - m_{\mathrm{P}_j}^*(t)\right) + m_{\mathrm{P_d}}^*(t), \tag{S2}$$

where the first term corresponds to the net effects of the treatment defined by the difference of the efficacy (percentage-improved EASI) between the j-th treatment ($m_j^*(t)$) and the corresponding placebo groups ($m_{\mathrm{P}_j}^*(t)$). This term adjusts for different efficacies in the placebo group across the clinical studies owing to differences in study participants' background, concomitant drugs, and sites of study (Wang et al., 2019). The second term corresponds to the placebo effects defined by the efficacy in the placebo group in the dupilumab clinical trial ($m_{\mathrm{P_d}}^*(t)$).

Normalized mean EASI score, $e_j(t)$, of the j-th treatment at t was calculated by the following:

$$e_j(t) = \frac{e_{\mathrm{d}}(0)\left(100 - m_j(t)\right)}{100}, \tag{S3}$$

where $e_{\mathrm{d}}(0)$, the reported baseline (before the trial), is the mean EASI score in the dupilumab clinical trial (Blauvelt et al., 2017), and $m_j(t)$ is the normalized percentage-improved EASI defined in equation (S2).

Normalized EASI-75 was estimated from the normalized percentage-improved EASI using a regression curve obtained from the relationship between the percentage-improved EASI and EASI-75 in clinical trials of multiple treatments (Blauvelt et al., 2017; Guttman-Yassky et al., 2020, 2019a; Kabashima et al., 2020; Silverberg et al., 2021; Simpson et al., 2019) (Supplementary Figure S3).

Model structure

The quantitative systems pharmacology model of *S. aureus*–targeted therapies (Figure 2) describes the dynamics of EASI score, skin barrier integrity, *S. aureus*, CoNS, IL-4/IL-13, and treatment effects. Those dynamics were formulated by equations (S4)–(S22) with six variables (Supplementary Table S2) and 26 parameters (Supplementary Table S3). This section introduces the equations.

t is the time after the start of treatments. The baseline levels of biological factors for our model (at $t = 0$) were obtained from the simulated steady-state level (after 1,000 weeks) without any intervention. We referred to the reported levels of biological factors without interventions of the treatments as the reference values for the baseline levels, assuming that the levels of the biological factors were stable before the start of treatments.

Biological factors. For accessory gene regulatory (agr) expression level, agr expression level, $a_{\mathrm{agr}}(t)$, of *S. aureus* is described (Supplementary Figure S4) by the following equation:

$$a_{\mathrm{agr}}(t) = \tanh\frac{k_1 a(t)}{1 + b_1 h(t)}, \tag{S4}$$

where $a(t)$ and $h(t)$ are *S. aureus* and CoNS levels ($\log_{10}$ colony-forming unit per cm^2), respectively, and b_1 describes the inhibitory strength for the agr expression by autoinducing peptides from CoNS (Williams et al., 2019).

For skin barrier integrity, the dynamics of the skin barrier integrity, $s(t)$, is described (Supplementary Figure S5) by the following:

$$\frac{ds(t)}{dt} = \frac{(1 - s(t))(k_2 + k_3)}{1 + b_2 c_4(t)} - s(t)\left\{d_1 + d_2 a_{\mathrm{agr}}(t)\right\}, \tag{S5}$$

where $c_4(t)$ is IL-4/IL-13 level; $s(t)$ is skin barrier integrity; k_2 and k_3 describe the recovery rate of skin barrier integrity through skin turnover and placebo effects, respectively; b_2 describes the inhibitory strength for recovery of skin barrier through IL-4/IL-13; and d_1 and d_2 describe the degradation rate of skin barrier through skin turnover and *S. aureus*, respectively.

The first term represents a recovery of skin barrier integrity by intrinsic skin turnover (with the recovery rate, k_2) and placebo effects (k_3). We assumed the maximal value of $s(t) = 1$ as a healthy state of skin barrier integrity (Supplementary Table S2) and thus modified the recovery rate by $1 - s(t)$. The placebo effect was applied to the simulations for both placebo- and drug-treated groups because placebo-treated patients improved on the EASI score (Blauvelt et al., 2017; Callewaert et al., 2020; Nakatsuji et al., 2021a), presumably because of the controlled care with concomitant drugs such as emollients during the clinical trials. The recovery of skin barrier integrity was assumed to be compromised by IL-4 and IL-13 (with the strength b_2) because they are shown to decrease FLG production (Howell et al., 2009; Seltmann et al., 2015), thereby inhibiting epidermal differentiation, and because they induce pruritus (Oetjen et al., 2017) and thus scratching of the skin.

The second term corresponds to the degradation of the skin barrier by skin turnover (with the degradation rate, d_1) and by *S. aureus,* which damages keratinocytes through phenol-soluble modulin-α and δ-toxin (d_2) (Syed et al., 2015). The latter (d_2) is agr dependent because the agr regulates the secretion of phenol-soluble modulin-α and δ-toxin from *S. aureus* (Queck et al., 2008).

For *S. aureus* and CoNS in the skin, the dynamics of *S. aureus* and CoNS in the skin, $a(t)$ and $h(t)$, are described (Supplementary Figure S6) by the following equations:

$$\frac{da(t)}{dt} = \frac{k_4}{1 + b_3 s(t)}\left(1 - \frac{a(t)}{a_{\max}}\right) - \left\{d_3 h(t) + \frac{d_4}{1 + b_4 c_4(t)} + d_5\right\} \tag{S6}$$

and

$$\frac{dh(t)}{dt} = k_5\left(1 - \frac{h(t)}{h_{\max}}\right) - \left\{d_6 a(t) + \frac{d_7}{1 + b_4 c_4(t)} + d_8\right\}, \tag{S7}$$

where k_4 and k_5 are the proliferation rates of *S. aureus* and CoNS, respectively; b_3 is the inhibitory coefficient for *S. aureus* proliferation through the skin barrier; b_4 is the

inhibitory strength for the elimination of *Staphylococci* through IL-4/IL-13; d_3 and d_4 are the killing rates of *S. aureus* through bacteriocins secreted from CoNS and through antimicrobial peptides (AMPs), respectively; d_5 is the elimination rate of *S. aureus* through turnover; d_6 and d_7 are the killing rates of CoNS through bacteriocins secreted from *S. aureus* and through AMPs, respectively; d_8 is the elimination rate of CoNS through turnover; and a_{max} and h_{max} are the maximal levels of *S. aureus* and CoNS, respectively. Equations (S6) and (S7) represent the logistic growth of $a(t)$ and $h(t)$ in $\log_{10}$ scale. We set $[a_{max}, h_{max}] = [7, 7]$ to cover the reported range of *S. aureus* levels (the reported maximal $\log_{10}$ level of *S. aureus* was 6) in the dupilumab clinical trial (Callewaert et al., 2020).

Equations (S6) and (S7) are relative growth rates on the basis of $\log_{10}$ scale ($\log_{10}$ colony-forming unit per cm^2). Their absolute growth rates can be described as follows:

$$a^*(t) = 10^{a(t)} \tag{S8}$$

$$h^*(t) = 10^{h(t)} \tag{S9}$$

$$\frac{da^*(t)}{dt} = \frac{da(t)}{dt} a^*(t) \ln 10$$

$$= \frac{k_4}{1 + b_3 s(t)} \left(1 - \frac{\log_{10} a^*(t)}{a_{max}}\right) a^*(t) \ln 10 - \left\{ d_3 \log_{10} h^*(t) + \frac{d_4}{1 + b_4 c_4(t)} + d_5 \right\} a^*(t) \ln 10 \tag{S10}$$

$$\frac{dh^*(t)}{dt} = \frac{dh(t)}{dt} h^*(t) \ln 10$$

$$= k_5 \left(1 - \frac{\log_{10} h^*(t)}{h_{max}}\right) h^*(t) \ln 10 - \left\{ d_6 \log_{10} a^*(t) + \frac{d_7}{1 + b_4 c_4(t)} + d_8 \right\} h^*(t) \ln 10 \tag{S11}$$

where $a^*(t)$ and $h^*(t)$ are absolute levels (colony-forming unit per cm^2) of *S. aureus* and CoNS in the skin, respectively. The first terms of equations (S10) and (S11) mean that we assumed that their logistic growth is based on the $\log_{10}$ scale of *S. aureus* and CoNS levels.

S. aureus and CoNS proliferate (with the rates k_4 and k_5), where healthy skin barrier integrity inhibits the proliferation of *S. aureus* by making skin pH acidic (with strength b_3), whereas skin pH does not affect those of CoNS (Kwaszewska et al., 2014; Lambers et al., 2006).

S. aureus and CoNS are killed by bacteriocins (released from *Staphylococci*) and AMP (released from keratinocytes) directly (Schröder, 2011). Bacteriocins exert antimicrobial activity against bacteria closely related to the producer strain but not against the producer strain itself (Jack et al.,1995); *S aureus* is killed by bacteriocins from CoNS (with strength d_3) (Nakatsuji et al., 2017) and AMP (d_4), and CoNS is killed by bacteriocins from *S. aureus* (d_6) and AMP (d_7). AMP release from keratinocytes is inhibited by IL-4 and IL-13 (Howell et al., 2006) (b_4). *S. aureus* and CoNS in the skin decrease owing to their natural death (d_5 and d_8).

We did not consider the influence of *S. aureus* on AMP because the experimental evidence is controversial: *S. aureus* increases AMP release from keratinocytes through pathways that are independent of the cytokines (Menzies and Kenoyer, 2005); *S. aureus* degrades AMP by aureolysin, which is a proteinase produced by *S. aureus* (Sieprawska-Lupa et al., 2004).

For IL-4 and IL-13, the dynamics of IL-4 and IL-13, $c_4(t)$, is described (Supplementary Figure S7) by the following equation:

$$\frac{dc_4(t)}{dt} = k_6 a_{agr}(t) + k_7 - d_9 c_4(t), \tag{S12}$$

where k_6 and k_7 are the secretion rate of IL-4/IL-13 through agr expression and other pathways, respectively, and d_9 is the elimination rate of IL-4/IL-13.

IL-4 and IL-13 are secreted from T helper 2 cells that are primed by dendritic cells specifically activated by *S. aureus*–derived wall teichoic acid (van Dalen et al., 2019) controlled by agr (Wanner et al., 2017) (with the rate k_6). There are other pathways releasing IL-4/IL-13, which were implicitly described as other effects (k_7).

For EASI score, the EASI score (ranging from 0 to 72) is calculated using the severity and the area scores of equally-weighted four AD signs (erythema, induration, excoriations, and lichenification) on four body regions (head/neck, trunk, upper limbs, and lower limbs) (Hanifin et al., 2001). In our model, the EASI score $e(t)$, is described (Supplementary Figure S8) by the following equation:

$$e(t) = 72 \frac{2a_{agr}(t) + 2(1 - s(t))}{4}, \tag{S13}$$

where 72 is the maximal EASI score. Scores derived from two AD signs (erythema and induration) and those from the remaining two signs (excoriations and lichenification) were surrogated by $a_{agr}(t)$ and $1 - s(t)$, respectively, as described below. We set $e(0) = 29.3$, the baseline EASI score of patients with AD in the dupilumab clinical trial, which was used as a reference value to normalize the EASI scores in all the clinical trials.

We assumed that the scores derived from erythema and induration are governed by $a_{agr}(t)$ because these two signs can be induced by *S. aureus* (Leung et al., 2000). We used $\log_{10}$ level of *S. aureus* to model $a_{agr}(t)$ in equation (S4) because the correlation between EASI score and $\log_{10}$ level

of *S. aureus* has been reported (Callewaert et al., 2020). Erythema is caused by inflammatory vasodilation by histamines (Grossmann et al., 1999). Histamine is released mainly from mast cells and basophils that are activated by detecting antigens, such as δ-toxin (Azimi et al., 2017) and *Staphylococcus* enterotoxins (Leung et al., 1993), released by *S. aureus* but not by CoNS (Becker et al., 2001). We associated the released histamine concentration with the antigen load in this model because the amount of histamine released depends more on the number of antigens than on that of antigen-specific IgE (Yamaguchi et al., 1999), although both antigens and antigen-specific IgE play a role in this process (Amin, 2012). A negligible contribution of IgE (compared with that of antigens) on the AD pathogenesis is also suggested by a lack of clinical efficacy shown for omalizumab (IgE-neutralizing anti–IgE antibody). Our model assumed that the histamine release by *S. aureus*–induced δ-toxin and enterotoxins depends on the agr expression level of *S. aureus* because autoinducing peptides from other strains regulate the secretion of δ-toxin and enterotoxins from *S. aureus* (Queck et al., 2008; Sihto et al., 2017). Scores for the other two AD signs—excoriations and lichenification—are surrogated by $1 - s(t)$, which describes the degree of damage of the skin barrier integrity, because excoriations and lichenification are caused by scratching (Bohl, 2019), which damages skin barrier integrity.

Treatment effects. Flucloxacillin, an antibiotic, kills the *Staphylococci* (*S. aureus* and CoNS). We described the effects of flucloxacillin (Supplementary Figure S9) on decreasing the *Staphylococci* by adding the killing rates of *Staphylococci* (d_{fa} and d_{fh}) in equations (S6) and (S7) as follows:

$$\frac{da(t)}{dt} = \frac{k_4}{1 + b_3 s(t)}\left(1 - \frac{a(t)}{a_{\max}}\right) - \left\{d_4 h(t) + \frac{d_5}{1 + b_4 c_4(t)} + d_6 + d_{\mathrm{fa}}\right\}, \tag{S14}$$

$$\frac{dh(t)}{dt} = k_5\left(1 - \frac{h(t)}{h_{\max}}\right) - \left\{d_6 a(t) + \frac{d_7}{1 + b_4 c_4(t)} + d_8 + d_{\mathrm{fh}}\right\}. \tag{S15}$$

*Sh*A9 is a specific strain of *S. hominis* that produces bacteriocins against *S. aureus* (Nakatsuji et al., 2021a) and inhibits agr expression of *S. aureus* (Williams et al., 2019). Although *Sh*A9 was screened on the basis of the selectivity of the bacteriocins against *S. aureus*, it still has antimicrobial activity against CoNS (Nakatsuji et al., 2017). We described those effects (Supplementary Figure S10) by adding the killing rates of *S. aureus* and CoNS (d_{A9a} and d_{A9h}) in equations (S6) and (S7) and the inhibitory strength for agr expression (b_{A9a}) in equation (S7) as follows:

$$\frac{da(t)}{dt} = \frac{k_4}{1 + b_3 s(t)}\left(1 - \frac{a(t)}{a_{\max}}\right) - \left\{d_4 h(t) + \frac{d_5}{1 + b_4 c_4(t)} + d_6 + d_{\mathrm{A9a}}\right\}, \tag{S16}$$

$$\frac{dh(t)}{dt} = k_5\left(1 - \frac{h(t)}{h_{\max}}\right) - \left\{d_6 a(t) + \frac{d_7}{1 + b_4 c_4(t)} + d_8 + d_{\mathrm{A9h}}\right\}, \tag{S17}$$

$$a_{\mathrm{agr}}(t) = \tanh\frac{k_1 a(t)}{(1 + b_1 h(t))(1 + b_{\mathrm{A9a}})}. \tag{S18}$$

The clinical trial of *Sh*A9 stratified the patients according to the sensitivity of *S. aureus* isolated from each patient to the bacteriocins of *Sh*A9. The colonized *S. aureus* was categorized as sensitive when the minimal inhibitory concentration of *Sh*A9-conditioned medium against *S. aureus* is <100% (percentage of the original conditioned medium) and as resistant when the minimal inhibitory concentration is >200% (Nakatsuji et al., 2021a). Hereafter, *Sh*A9 is applied to patients colonized with *S. aureus* sensitive to *Sh*A9 bacteriocins and is referred to as *Sh*A9 sensitive and to those with *S. aureus* resistant to *Sh*A9 bacteriocins and is referred to as *Sh*A9 resistant. We modeled the different sensitivity of *S. aureus* to the bacteriocins of *Sh*A9 as follows:

$$d_{\mathrm{A9a}} = \begin{cases} d_{\mathrm{A9a\_s}}, & \textit{if } Sh\mathrm{A9} - \text{sensitive} \\ d_{\mathrm{A9a\_r}}, & \textit{if } Sh\mathrm{A9} - \text{resistant}\,. \end{cases} \tag{S19}$$

Effects of *Sh*A9 were applied in both dosing and follow-up periods in the simulation because the measured amount of *Sh*A9 remained higher than the baseline levels during the follow-up periods in the clinical trial (Nakatsuji et al., 2021a).

For dupilumab, we described the effects of dupilumab (Supplementary Figure S11) that inhibit the signaling of IL-4 and IL-13 by scaling the concentrations of IL-4 and IL-13. Effective concentrations of the IL-4 and IL-13 in the skin at t, $c_4(t)$, was modeled by the following equation:

$$c_4(t) = (1 - r_{\mathrm{inhibit}})c_4^*(t), \tag{S20}$$

$$r_{\mathrm{inhibit}} = \frac{d_{\mathrm{skin}}}{\mathrm{IC}_{50} + d_{\mathrm{skin}}}, \tag{S21}$$

$$d_{\mathrm{skin}} = r_{\mathrm{skin/serum}} d_{\mathrm{serum}}, \tag{S22}$$

where $c_4^*(t)$ is the concentration of IL-4 and IL-13 in the skin at t, r_{inhibit} is the rate of IL-4 and IL-13 inhibition in the dupilumab treatment, d_{skin} is the concentration of dupilumab in the skin, IC_{50} is the half-maximal inhibitory concentration of dupilumab against IL-4 and IL-13, $r_{\mathrm{skin/serum}}$ is the ratio of dupilumab concentration in the skin to that in serum, and d_{serum} is the mean concentration of dupilumab in the serum. We adopted $r_{\mathrm{skin/serum}} = 0.157$ for dupilumab on the basis of the estimated ratio of antibody concentration in the skin to that in the plasma (Shah et al., 2013). Values of IC_{50} (<0.01 mcg/ml for IL-4 and 0.01 mcg/ml for IL-13) and

d_{serum} (183 mcg/ml) were obtained from reported results of in vitro assay and the reported pharmacokinetic data of the adopted dose regimen (Table 1) in clinical trials (Le Floc'h et al., 2020). With these values, $r_{inhibit}$ was calculated as 0.99.

Optimizing model parameters to reproduce clinical data

We optimized 52 parameters (μ_i and σ_i) that define the distributions of the 26 model parameters (Supplementary Table S3) so that the model reproduces the following clinical data consisting of 108 reference values:

1. mean values and coefficient of variation (CV) of four biological factors—IL-4/IL-13, *S. aureus*, CoNS, and the EASI score—without interventions of the treatments (Supplementary Table S2) (2 indices × 4 factors = 8 reference values);
2. the EASI score and EASI-75 in the clinical trials (Figure 1) (2 indices × 5 interventions × 4–7 time points/intervention = 56 reference values); and
3. mean values and CV of *S. aureus* levels in the clinical trials (Figure 1) (2 indices × 5 interventions × 4–5 time points/intervention = 44 reference values).

We searched the parameters that minimize the cost function, J, defined by the following equation:

$$J = w_1 J_1 + w_2 J_2 + w_3 J_3 + w_4 J_4 + w_5 J_5 + w_6 J_6, \tag{S23}$$

where

$$J_1 = \sqrt{\frac{1}{4}\sum_{l=1}^{4}\left(b_{\mathrm{mean},l} - \widehat{b}_{\mathrm{mean},l}\right)^2}, \tag{S24}$$

$$J_2 = \sqrt{\frac{1}{4}\sum_{l=1}^{4}\left(b_{\mathrm{CV},l} - \widehat{b}_{\mathrm{CV},l}\right)^2}, \tag{S25}$$

$$J_3 = \sqrt{\frac{1}{5}\sum_{j=1}^{5}\left\{\frac{1}{m_{\mathrm{last},j}}\sum_{m=1}^{m_{\mathrm{last},j}}\left(e_j(t_m) - \widehat{e}_j(t_m)\right)^2\right\}}, \tag{S26}$$

$$J_4 = \sqrt{\frac{1}{5}\sum_{j=1}^{5}\left\{\frac{1}{m_{\mathrm{last},j}}\sum_{m=1}^{m_{\mathrm{last},j}}\left(e_{75,j}(t_m) - \widehat{e}_{75,j}(t_m)\right)^2\right\}}. \tag{S27}$$

$$J_5 = \sqrt{\frac{1}{5}\sum_{j=1}^{5}\left\{\frac{1}{m_{\mathrm{last},j}}\sum_{m=1}^{m_{\mathrm{last},j}}\left(a_j(t_m) - \widehat{a}_j(t_m)\right)^2\right\}}, \tag{S28}$$

and

$$J_6 = \sqrt{\frac{1}{5}\sum_{j=1}^{5}\left\{\frac{1}{m_{\mathrm{last},j}}\sum_{m=1}^{m_{\mathrm{last},j}}\left(a_{\mathrm{CV},j}(t_m) - \widehat{a}_{\mathrm{CV},j}(t_m)\right)^2\right\}}. \tag{S29}$$

The terms, J_1 and J_2, are the root mean squared errors of mean values and CV of baseline levels of biological factors, respectively; J_3 and J_4 are the root mean squared errors of the EASI score and EASI-75, respectively; and J_5 and J_6 are the root mean squared errors of mean values and CV of *S. aureus* levels, respectively. w_1 to w_6 are the weighting coefficients. $b_{\mathrm{mean},l}$ and $b_{\mathrm{CV},l}$ are the reference values for the mean value and the CV of the baseline levels of the l-th biological factor (l = 1, 2, 3, 4). $\widehat{b}_{\mathrm{mean},l}$ and $\widehat{b}_{\mathrm{CV},l}$ are the corresponding simulated values at the steady state (after 1,000 weeks, among 1,000 virtual patients). $e_j(t_m)$, $e_{75,j}(t_m)$, $a_j(t_m)$, and $a_{\mathrm{CV},j}(t_m)$ are the reference values of the EASI score, EASI-75, mean *S. aureus* levels, and CV of *S. aureus* levels using the j-th intervention (j = 1, 2, 3, 4, 5) at time t_m (m = 1, …, $m_{\mathrm{last},j}$). $\widehat{e}_j(t_m)$, $\widehat{e}_{75,j}(t_m)$, $\widehat{a}_j(t_m)$, and $\widehat{a}_{\mathrm{CV},j}(t_m)$ are the corresponding simulated values. We used $[w_1, w_2, w_3, w_4, w_5, w_6]$ = [50, 10, 50, 50, 1000, 1] with larger weights on some terms (e.g., J_5) that tended to have smaller fitting errors.

The parameters were optimized using differential evolution (Storn and Price, 1997), which is an effective method for global optimization of a large number of parameters. The conditions for differential evolution were set as follows on the basis of manual trial and error: mutation constant = 0.5, crossover constant = 0.7, strategy = DE/best/1/bin, number of population vectors = 52, number of function evaluations = 15,652, number of evaluated generations = 300, and ranges of parameters searched (as shown in Supplementary Table S3).

The J reached a plateau value, 569, after the iterative evaluations (Supplementary Figure S12). The model fitness was confirmed visually by comparing the reference data with the simulated data (Figure 3).

Sensitivity analysis

We conducted a global sensitivity analysis of the model parameters with respect to the percentage-improved EASI. We produced 1,000 virtual patients by varying the 26 parameters that represent their pathophysiological backgrounds, using Latin hypercube sampling and computed partial rank correlation coefficient (PRCC) (Marino et al., 2008) between each parameter and the percentage-improved EASI of each treatment. Latin hypercube sampling is a sampling method to explore the entire space of multidimensional parameters efficiently, and PRCC represents a rank correlation coefficient that is controlled for confounding effects that could lead to detecting pseudocorrelations. The evaluated ranges of $\ln k_i$ were $[\mu_i - \sigma_i, \mu_i + \sigma_i]$. The P-values for the PRCC were adjusted for multiple testing with the Bonferroni procedure, where a significant level of adjusted $P < 0.05$ with an absolute value >0.1 was used.

Influence of model parameters on efficacy of placebo. Eight model parameters had a significant PRCC with the

percentage-improved EASI by placebo (Supplementary Figure S13).

Two of the eight parameters were skin barrier related (k_3 and b_2). A higher k_3 results in stronger recovery of skin barrier through placebo effects, thereby achieving a higher percentage-improve EASI. A higher b_2 inhibits the recovery of skin barrier more strongly, weakening the recovery of the skin barrier by placebo effects, thereby showing lower percentage-improved EASI.

The remaining six parameters were agr related (k_1, k_4, k_5, b_1, d_5, and d_8). Higher b_1, k_5, and d_5 and lower k_1, k_4, and d_8 result in a lower baseline level of agr expression by decreasing agr expression levels (k_1 and b_1) and *S. aureus* levels (k_4 and d_5) or increasing CoNS levels (k_5 and d_8). A lower level of agr expression means that the percentage-improved EASI score is more sensitive to the changes in the skin barrier integrity that is achieved by placebo effects because we modeled an EASI score as a weighted mean of agr expression and skin barrier integrity (equation [S13]).

These influences were observed in not only the placebo groups but also in drug-treated groups because the placebo effects were considered in both placebo- and drug-treated groups in the simulation.

Influence of model parameters on efficacy of dupilumab. Six model parameters had a significant PRCC with the percentage-improved EASI by dupilumab (Supplementary Figure S13). All the six parameters were agr related (k_1, k_4, k_5, d_4, d_5, and d_8). Higher k_5, d_4, and d_5 and the lower k_1, k_4, and d_8 result in a lower baseline level of agr expression owing to a decrease in agr expression (k_1) and in *S. aureus* levels (k_4, d_4, and d_5) or to an increase in CoNS levels (k_5 and d_8). A lower level of agr expression means that the percentage-improved EASI score is more sensitive to the changes in the skin barrier integrity that is achieved by placebo effects and dupilumab (inhibiting skin barrier damage from IL-4/IL-13) because we modeled an EASI score as a weighted mean of agr expression and skin barrier integrity (equation [S13]).

Two skin barrier–related parameters (k_3 and b_2) had a significant PRCC with the percentage-improved EASI by placebo but not by dupilumab, which includes placebo effects in our simulation. It may be because the recovery of the skin barrier by dupilumab overweighed that by placebo effects, and therefore the placebo effects became negligible in dupilumab treatment.

Influence of model parameters on efficacy of* Sh*A9 sensitive. Seven model parameters had a significant PRCC with the percentage-improved EASI by *Sh*A9 sensitive (Supplementary Figure S13). Two of the seven parameters were skin barrier related (k_3 and b_2) and correspond to placebo effects because they had a significant PRCC with the percentage-improved EASI by placebo ("Selection of clinical studies for development of the quantitative systems pharmacology" model in Supplementary Materials and Methods). The other two parameters were bactericidal strengths of *Sh*A9 (d_{A9a_s} and d_{A9h}). A higher d_{A9a_s} and a lower d_{A9h} result in stronger killing of *S. aureus* and weaker killing of CoNS, respectively, thereby achieving a higher percentage-improved EASI.

The remaining three parameters were agr related (k_4, k_5, and d_8). As described in "Selection of clinical studies for development of the quantitative systems pharmacology model" in Supplementary Materials and Methods, a lower k_4 showed a higher percentage-improved EASI in placebo treatment. A higher d_8 and a lower k_5 result in a lower baseline level of CoNS. The lower level of CoNS lessens the impact of killing CoNS by *Sh*A9 on the increase of agr expression. The smaller increase in agr expression resulted in the weaker detrimental effects of *Sh*A9 on EASI scores, thereby showing a higher percentage-improved EASI.

The influences of d_8 and k_5 (i.e., a baseline level of CoNS) on the percentage-improved EASI were in opposite directions, depending on whether the drugs kill CoNS (e.g., *Sh*A9 and flucloxacillin) or not (e.g., placebo and dupilumab). A higher baseline level of CoNS makes a lower baseline level of agr expression. The lower level of agr expression means that the percentage-improved EASI score is more sensitive to the changes in the skin barrier integrity that is achieved by placebo and dupilumab because we modeled an EASI score as a weighted mean of agr expression and skin barrier integrity (equation [S13]). In contrast, a lower level of CoNS lessens the impact of killing CoNS by *Sh*A9 on the increase of agr expression. The smaller increase in agr expression results in weaker detrimental effects of *Sh*A9 and flucloxacillin on EASI scores, thereby showing a higher percentage-improved EASI.

b_{A9s} (inhibitory strength for agr expression of *S. aureus* by *Sh*A9) had no significant influence on the percentage-improved EASI (Supplementary Figure S13) because the inhibitory strength of *Sh*A9 for agr expression of *S. aureus* is so weak in this model (i.e., a small μ_i of b_{A9s}) that the sensitivity analysis evaluated a narrow range of inhibition levels of agr expression (the evaluated range of b_{A9s} was 0.25–0.43, 20–30% around the nominal value). In contrast, the inhibitory level of agr expression through hypothetical *S. aureus*–targeted therapy had a significant influence on EASI-75 (Figure 5) because it evaluated a whole range of inhibition levels of agr expression (0–100%).

Influence of model parameters on efficacy of* Sh*A9 resistant. Six model parameters had a significant PRCC with the percentage-improved EASI by *Sh*A9 resistant (Supplementary Figure S13). Two of the six parameters were skin barrier related (k_3 and b_2) and correspond to placebo effects because they had a significant PRCC with the percentage-improved EASI by placebo ("Selection of clinical studies for development of the quantitative systems pharmacology model" in Supplementary Materials and Methods). A parameter, d_{A9h}, is the bactericidal strength of *Sh*A9 on CoNS. A lower d_{A9h} results in weaker killing of CoNS, thereby achieving a higher percentage-improved EASI.

The remaining three parameters were agr related (k_4, d_5, and d_8). As described in "Selection of clinical studies for development of the quantitative systems pharmacology model" in Supplementary Materials and Methods, a higher d_5 and lower k_4 resulted in stronger skin barrier recovery by placebo effects and thereby showed a higher percentage-improved EASI. A higher d_8 results in a lower baseline level of CoNS. The lower level of CoNS lessens the impact of

CoNS killing by *Sh*A9 on the increase of agr expression. The smaller increase in agr expression resulted in weaker detrimental effects of *Sh*A9 on EASI scores, thereby showing a higher percentage-improved EASI. *Sh*A9 resistant and *Sh*A9 sensitive showed similar results except for k_5, d_5, and d_{A9a_s}/d_{A9a_r}; the discrepancy stems from the difference in bactericidal strengths on *S. aureus*.

Influence of model parameters on efficacy of flucloxacillin. Eight model parameters had a significant PRCC with the percentage-improved EASI by flucloxacillin (Supplementary Figure S13). Two of the eight parameters were skin barrier related (k_3 and b_2) and correspond to placebo effects ("Selection of clinical studies for the development of the quantitative systems pharmacology model" in Supplementary Materials and Methods). The two parameters were bactericidal strengths of flucloxacillin (d_{fa} and d_{fh}). A higher d_{fa} and a lower d_{fh} result in stronger killing of *S. aureus* and weaker killing of CoNS, respectively, thereby achieving a higher percentage-improved EASI.

The remaining four parameters were agr related (k_4, k_5, d_5, and d_8). As described in "Selection of clinical studies for the development of the quantitative systems pharmacology model" in Supplementary Materials and Methods, a higher d_5 and a lower k_4 result in stronger recovery of skin barrier through placebo effects, thereby showing a higher percentage-improved EASI. A higher d_8 and a lower k_5 have a lower baseline level of CoNS. The lower level of CoNS lessens the impact of killing CoNS by flucloxacillin on the increase of agr expression. The smaller increase in agr expression resulted in weaker detrimental effects of *Sh*A9 on EASI scores, thereby showing a higher percentage-improved EASI.

SUPPLEMENTARY REFERENCES

Amin K. The role of mast cells in allergic inflammation. Respir Med 2012;106:9–14.

Azimi E, Reddy VB, Lerner EA. Brief communication: MRGPRX2, atopic dermatitis and red man syndrome. Itch (Phila) 2017;2:e5.

Becker K, Haverkämper G, von Eiff C, Roth R, Peters G. Survey of staphylococcal enterotoxin genes, exfoliative toxin genes, and toxic shock syndrome toxin 1 gene in non-Staphylococcus aureus species. Eur J Clin Microbiol Infect Dis 2001;20:407–9.

Blauvelt A, de Bruin-Weller M, Gooderham M, Cather JC, Weisman J, Pariser D, et al. Long-term management of moderate-to-severe atopic dermatitis with dupilumab and concomitant topical corticosteroids (LIBERTY AD CHRONOS): a 1-year, randomised, double-blinded, placebo-controlled, phase 3 trial. Lancet 2017;389:2287–303.

Bohl T. Lichenification superimposed on an underlying preceding pruritic disease. In: Bornstein J, editor. Vulvar disease. Cham, Switzerland: Springer; 2019. p. 153–5.

Callewaert C, Nakatsuji T, Knight R, Kosciolek T, Vrbanac A, Kotol P, et al. IL-4Rα blockade by dupilumab decreases Staphylococcus aureus colonization and increases microbial diversity in atopic dermatitis. J Invest Dermatol 2020;140:191–202.e7.

de Wit J, Totté JEE, van Mierlo MMF, et al. Endolysin treatment against Staphylococcus aureus in adults with atopic dermatitis: A randomized controlled trial. J Allergy Clin Immunol 2019;144:860–3.

D'Ippolito D, Pisano M. Dupilumab (Dupixent): an interleukin-4 receptor antagonist for atopic dermatitis. P T 2018;43:532–5.

dos Santos Nascimento J, Fagundes PC, de Paiva Brito MA, dos Santos KR, do Carmo de Freire Bastos M. Production of bacteriocins by coagulase-negative staphylococci involved in bovine mastitis. Vet Microbiol 2005;106:61–71.

Ewing CI, Ashcroft C, Gibbs AC, Jones GA, Connor PJ, David TJ. Flucloxacillin in the treatment of atopic dermatitis. Br J Dermatol 1998;138:1022–9.

George SM, Karanovic S, Harrison DA, Rani A, Birnie AJ, Bath-Hextall FJ, et al. Interventions to reduce Staphylococcus aureus in the management of eczema. Cochrane Database Syst Rev 2019;2019:CD003871.

Foelster Holst R, Reitamo S, Yankova R, Worm M, Kadurina M, Thaci D, et al. The novel protease inhibitor SRD441 ointment is not effective in the treatment of adult subjects with atopic dermatitis: results of a randomized, vehicle-controlled study [published correction appears in Allergy 2011;66:306]. Allergy 2010;65:1594–9.

Grossmann M, Jamieson MJ, Kirch W. Histamine response and local cooling in the human skin: involvement of H1- and H2-receptors. Br J Clin Pharmacol 1999;48:216–22.

Gueniche A, Knaudt B, Schuck E, Volz T, Bastien P, Martin R, et al. Effects of nonpathogenic gram-negative bacterium Vitreoscilla filiformis lysate on atopic dermatitis: a prospective, randomized, double-blind, placebo-controlled clinical study. Br J Dermatol 2008;159:1357–63.

Guttman-Yassky E, Bissonnette R, Ungar B, Suárez-Fariñas M, Ardeleanu M, Esaki H, et al. Dupilumab progressively improves systemic and cutaneous abnormalities in patients with atopic dermatitis. J Allergy Clin Immunol 2019a;143:155–72.

Guttman-Yassky E, Blauvelt A, Eichenfield LF, Paller AS, Armstrong AW, Drew J, et al. Efficacy and Safety of lebrikizumab, a High-Affinity interleukin 13 Inhibitor, in Adults With Moderate to Severe Atopic Dermatitis: A Phase 2b Randomized Clinical Trial. JAMA Dermatol 2020;156:411–20.

Guttman-Yassky E, Pavel AB, Zhou L, Estrada YD, Zhang N, Xu H, et al. GBR 830, an anti-OX40, improves skin gene signatures and clinical scores in patients with atopic dermatitis. J Allergy Clin Immunol 2019b;144:482–93.e7.

Hanifin JM, Thurston M, Omoto M, Cherill R, Tofte SJ, Graeber M. The eczema area and severity index (EASI): assessment of reliability in atopic dermatitis. EASI Evaluator Group. Exp Dermatol 2001;10:11–8.

Howell MD, Boguniewicz M, Pastore S, Novak N, Bieber T, Girolomoni G, et al. Mechanism of HBD-3 deficiency in atopic dermatitis. Clin Immunol 2006;121:332–8.

Howell MD, Kim BE, Gao P, Grant AV, Boguniewicz M, DeBenedetto A, et al. Cytokine modulation of atopic dermatitis filaggrin skin expression. J Allergy Clin Immunol 2009;124:R7–12.

Jack RW, Tagg JR, Ray B. Bacteriocins of gram-positive bacteria. Microbiol Rev 1995;59:171–200.

Kabashima K, Matsumura T, Komazaki H, Kawashima M. Nemolizumab-JP01 Study Group. Trial of Nemolizumab and topical agents for atopic dermatitis with pruritus. N Engl J Med 2020;383:141–50.

Koppes SA, Brans R, Ljubojevic Hadzavdic S, Frings-Dresen MH, Rustemeyer T, Kezic S. Stratum corneum tape stripping: monitoring of inflammatory mediators in atopic dermatitis patients using topical therapy. Int Arch Allergy Immunol 2016;170:187–93.

Kwaszewska A, Sobiś-Glinkowska M, Szewczyk EM. Cohabitation—relationships of corynebacteria and staphylococci on human skin. Folia Microbiol (Praha) 2014;59:495–502.

Lambers H, Piessens S, Bloem A, Pronk H, Finkel P. Natural skin surface pH is on average below 5, which is beneficial for its resident flora. Int J Cosmet Sci 2006;28:359–70.

Lane P. Handling drop-out in longitudinal clinical trials: a comparison of the LOCF and MMRM approaches. Pharm Stat 2008;7:93–106.

Le Floc'h A, Allinne J, Nagashima K, Scott G, Birchard D, Asrat S, et al. Dual blockade of IL-4 and IL-13 with dupilumab, an IL-4Rα antibody, is required to broadly inhibit type 2 inflammation. Allergy 2020;75:1188–204.

Leung DY. Atopic dermatitis: new insights and opportunities for therapeutic intervention. J Allergy Clin Immunol 2000;105:860–76.

Leung DY, Harbeck R, Bina P, Reiser RF, Yang E, Norris DA, et al. Presence of IgE antibodies to staphylococcal exotoxins on the skin of patients with atopic dermatitis. Evidence for a new group of allergens. J Clin Invest 1993;92:1374–80.

Leung TH, Zhang LF, Wang J, Ning S, Knox SJ, Kim SK. Topical hypochlorite ameliorates NF-κB-mediated skin diseases in mice. J Clin Invest 2013;123:5361–70.

Marino S, Hogue IB, Ray CJ, Kirschner DE. A methodology for performing global uncertainty and sensitivity analysis in systems biology. J Theor Biol 2008;254:178–96.

Menzies BE, Kenoyer A. Staphylococcus aureus infection of epidermal keratinocytes promotes expression of innate antimicrobial peptides. Infect Immun 2005;73:5241–4.

Miyano T, Irvine AD, Tanaka RJ. A mathematical model to identify optimal combinations of drug targets for dupilumab poor responders in atopic dermatitis. Allergy 2021;77:582–94.

Myles IA, Earland NJ, Anderson ED, Moore IN, Kieh MD, Williams KW, et al. First-in-human topical microbiome transplantation with Roseomonas mucosa for atopic dermatitis. JCI Insight 2018;3:e120608.

Nakatsuji T, Chen TH, Narala S, Chun KA, Two AM, Yun T, et al. Antimicrobials from human skin commensal bacteria protect against Staphylococcus aureus and are deficient in atopic dermatitis. Sci Transl Med 2017;9:eaah4680.

Nakatsuji T, Gallo RL, Shafiq F, Tong Y, Chun K, Butcher AM, et al. Use of autologous bacteriotherapy to treat *Staphylococcus aureus* in patients with atopic dermatitis: A randomized double-blind clinical trial. JAMA Dermatol 2021b;157:978–82.

Nakatsuji T, Hata TR, Tong Y, Cheng JY, Shafiq F, Butcher AM, et al. Development of a human skin commensal microbe for bacteriotherapy of atopic dermatitis and use in a phase 1 randomized clinical trial. Nat Med 2021a;27:700–9.

Oetjen LK, Mack MR, Feng J, Whelan TM, Niu H, Guo CJ, et al. Sensory neurons co-opt classical immune signaling pathways to mediate chronic itch. Cell 2017;171:217–28.e13.

Queck SY, Jameson-Lee M, Villaruz AE, Bach TH, Khan BA, Sturdevant DE, et al. RNAIII-independent target gene control by the agr quorum-sensing system: insight into the evolution of virulence regulation in Staphylococcus aureus. Mol Cell 2008;32:150–8.

Sawada Y, Tong Y, Barangi M, Hata T, Williams MR, Nakatsuji T, et al. Dilute bleach baths used for treatment of atopic dermatitis are not antimicrobial in vitro [published correction appears in J Allergy Clin Immunol 2019;144:1456]. J Allergy Clin Immunol 2019;143:1946–8.

Schröder JM. Antimicrobial peptides in healthy skin and atopic dermatitis. Allergol Int 2011;60:17–24.

Seltmann J, Roesner LM, von Hesler FW, Wittmann M, Werfel T. IL-33 impacts on the skin barrier by downregulating the expression of filaggrin. J Allergy Clin Immunol 2015;135:1659–61.e4.

Shah DK, Betts AM. Antibody biodistribution coefficients: inferring tissue concentrations of monoclonal antibodies based on the plasma concentrations in several preclinical species and human. mAbs 2013;5:297–305.

Sieprawska-Lupa M, Mydel P, Krawczyk K, Wójcik K, Puklo M, Lupa B, et al. Degradation of human antimicrobial peptide LL-37 by Staphylococcus aureus-derived proteinases. Antimicrob Agents Chemother 2004;48:4673–9.

Sihto HM, Stephan R, Engl C, Chen J, Johler S. Effect of food-related stress conditions and loss of agr and sigB on seb promoter activity in S. aureus. Food Microbiol 2017;65:205–12.

Silverberg JI, Toth D, Bieber T, Alexis AF, Elewski BE, Pink AE, et al. Tralokinumab plus topical corticosteroids for the treatment of moderate-to-severe atopic dermatitis: results from the double-blind, randomized, multicentre, placebo-controlled phase III ECZTRA 3 trial. Br J Dermatol 2021;184:450–63.

Simpson EL, Bieber T, Guttman-Yassky E, Beck LA, Blauvelt A, Cork MJ, et al. Two phase 3 trials of dupilumab versus placebo in atopic dermatitis. N Engl J Med 2016;375:2335–48.

Simpson EL, Parnes JR, She D, Crouch S, Rees W, Mo M, et al. Tezepelumab, an anti-thymic stromal lymphopoietin monoclonal antibody, in the treatment of moderate to severe atopic dermatitis: a randomized phase 2a clinical trial. J Am Acad Dermatol 2019;80:1013–21.

Storn R, Price K. Differential evolution–a simple and efficient heuristic for global optimization over continuous spaces. J Glob Optim 1997;11:341–59.

Syed AK, Reed TJ, Clark KL, Boles BR, Kahlenberg JM. Staphlyococcus aureus phenol-soluble modulins stimulate the release of proinflammatory cytokines from keratinocytes and are required for induction of skin inflammation [published correction appears in Infect Immun 2015;83:4450]. Infect Immun 2015;83:3428–37.

van Dalen R, De La Cruz Diaz JS, Rumpret M, Fuchsberger FF, van Teijlingen NH, Hanske J, et al. Langerhans cells sense *Staphylococcus aureus* wall teichoic acid through Langerin to induce inflammatory responses. mBio 2019;10:e00330–19.

Wang EB, Shen L, Heathman M, Chan JR. Incorporating placebo response in quantitative systems pharmacology models. CPT Pharmacometrics Syst Pharmacol 2019;8:344–6.

Wanner S, Schade J, Keinhörster D, Weller N, George SE, Kull L, et al. Wall teichoic acids mediate increased virulence in Staphylococcus aureus. Nat Microbiol 2017;2:16257.

Williams MR, Costa SK, Zaramela LS, Khalil S, Todd DA, Winter HL, et al. Quorum sensing between bacterial species on the skin protects against epidermal injury in atopic dermatitis. Sci Transl Med 2019;11:eaat8329.

Wong SM, Ng TG, Baba R. Efficacy and safety of sodium hypochlorite (bleach) baths in patients with moderate to severe atopic dermatitis in Malaysia. J Dermatol 2013;40:874–80.

Yamaguchi M, Sayama K, Yano K, Lantz CS, Noben-Trauth N, Ra C, et al. IgE enhances Fc epsilon receptor I expression and IgE-dependent release of histamine and lipid mediators from human umbilical cord blood-derived mast cells: synergistic effect of IL-4 and IgE on human mast cell Fc epsilon receptor I expression and mediator release. J Immunol 1999;162:5455–65.

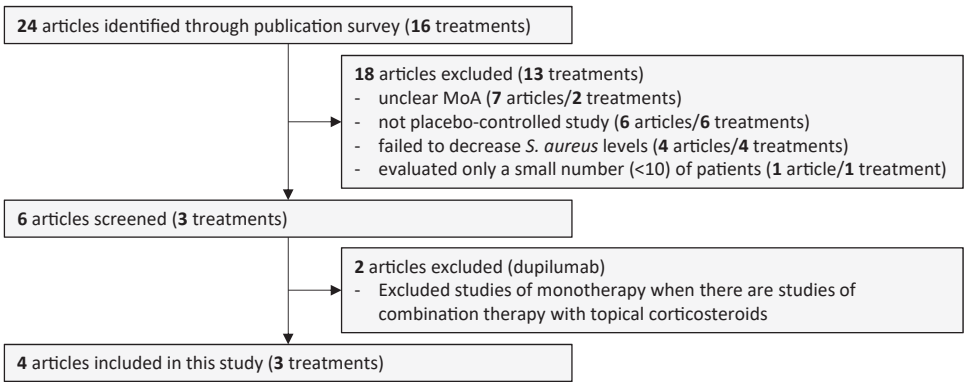

Supplementary Figure S1. Clinical studies selection process. MoA, mechanism of action.

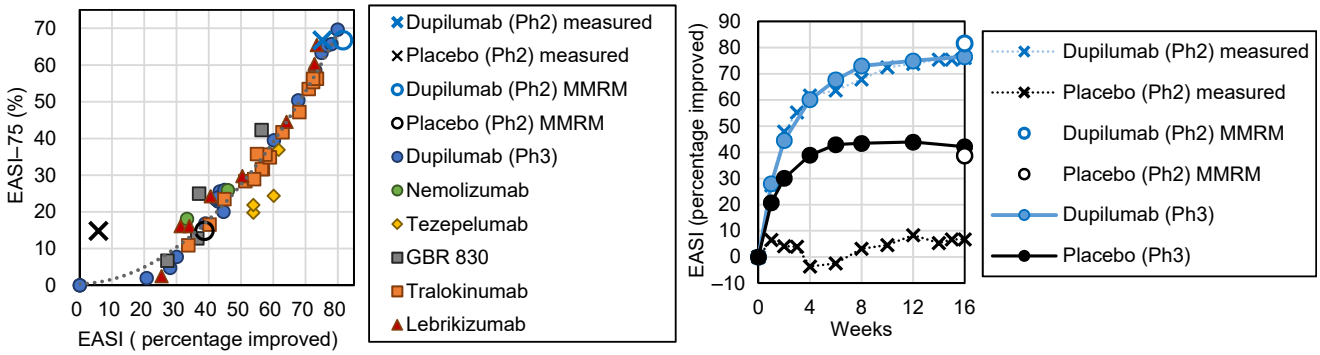

Supplementary Figure S2. Percentage-improved EASI reported in different clinical trials. Left: the relationship between the percentage-improved EASI and EASI-75. The placebo data measured in week 16 in a dupilumab Ph2 study (Callewaert et al., 2020) (a black cross) deviate from the data from other clinical trials (all available time points of both drug- and placebo-treated groups in dupilumab Ph3 [Blauvelt et al., 2017], nemolizumab [Kabashima et al., 2020], tezepelumab [Simpson et al., 2019], GBR 830 [Guttman-Yassky et al., 2019b], lebrikizumab [Guttman-Yassky et al., 2020b], and tralokinumab [Silverberg et al., 2021] studies) and the relationship between the percentage-improved EASI estimated by MMRM and EASI-75 measured in week 16 in a dupilumab Ph2 study (Callewaert et al., 2020) (a blue open circle for dupilumab-treated group and a black open circle for placebo-treated group). Right: the percentage-improved EASI in dupilumab Ph2 and Ph3 studies. The estimated percentage-improved EASI by MMRM at week 16 in Ph2 (Callewaert et al., 2020) (open circles) is comparable with the percentage-improved EASI in Ph3 (Blauvelt et al., 2017) (filled circles) for both dupilumab- and placebo-treated groups. EASI, Eczema Area and Severity Index; MMRM, mixed-effect model repeated measure; Ph, phase.

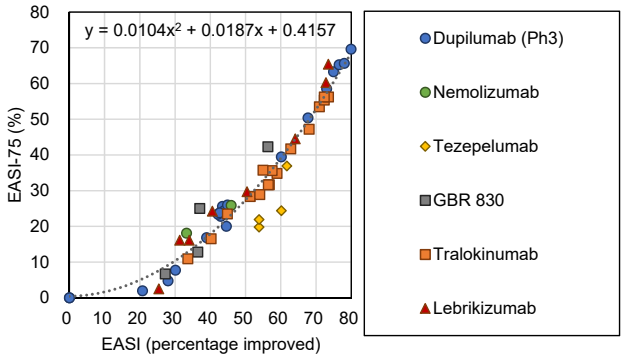

Supplementary Figure S3. EASI-75 was estimated from percentage-improved EASI using a regression curve. The regression curve was obtained using the reported percentage-improved EASI and EASI-75 in clinical trials of multiple treatments (all available time points of both drug- and placebo-treated groups in dupilumab [Blauvelt et al., 2017], nemolizumab [Kabashima et al., 2020], tezepelumab [Simpson et al., 2019], GBR 830 [Guttman-Yassky et al., 2019b], lebrikizumab [Guttman-Yassky et al., 2020], and tralokinumab [Silverberg et al., 2021]). EASI, Eczema Area and Severity Index; Ph, phase.

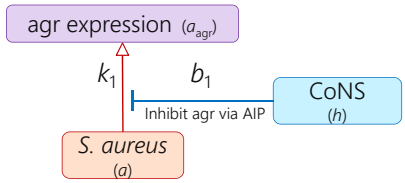

Supplementary Figure S4. Expression of agr is regulated by *Staphylococcus aureus* and CoNS. agr, accessory gene regulatory; AIP, autoinducing peptide; CoNS, coagulase-negative *Staphylococcus*.

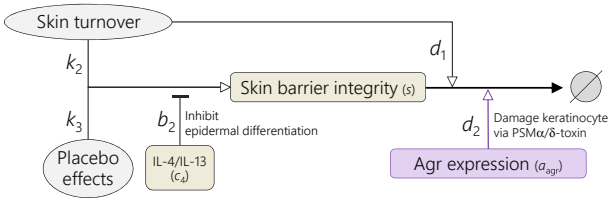

Supplementary Figure S5. Skin barrier integrity is regulated by skin turnover, placebo effects, IL-4/IL-13, and agr expression. Squared and oval symbols represent the model variables and implicit factors in our model, respectively. agr, accessory gene regulatory.

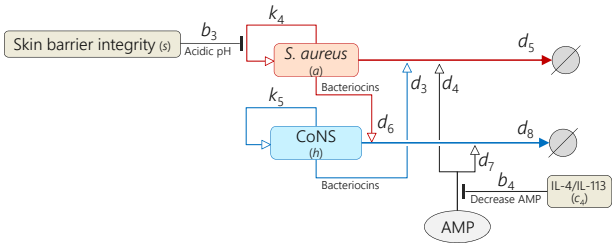

Supplementary Figure S6. *Staphylococcus aureus* and CoNS levels regulate each other. Squared and oval symbols represent the model variables and implicit factors in our model, respectively. AMP, antimicrobial peptide; CoNS, coagulase-negative *Staphylococcus*.

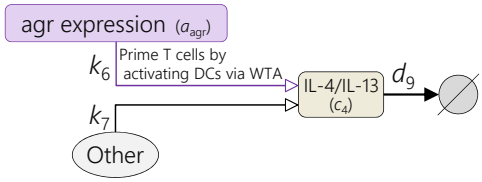

Supplementary Figure S7. IL-4/IL-13 level is regulated by agr expression and other factors. Squared and oval symbols represent model variables and implicit factors in our model, respectively. agr, accessory gene regulatory; DC, dendritic cell; WTA, wall teichoic acid.

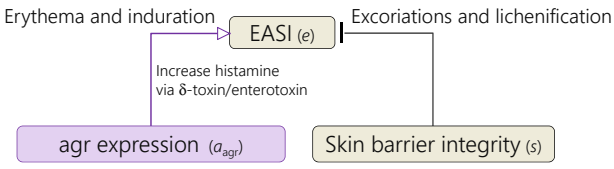

Supplementary Figure S8. EASI score was calculated from agr expression and skin barrier integrity. agr, accessory gene regulatory; EASI, Eczema Area and Severity Index.

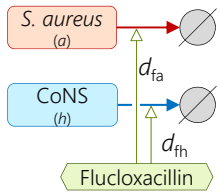

Supplementary Figure S9. Effects of flucloxacillin. Squared and hexagon symbols represent model variables and treatment in our model, respectively. CoNS, coagulase-negative *Staphylococcus*.

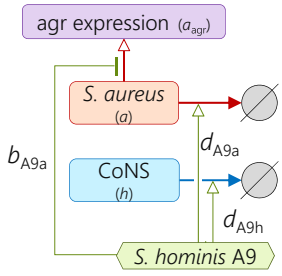

Supplementary Figure S10. Effects of *Staphylococcus hominis* A9. Squared and hexagon symbols represent model variables and treatment in our model, respectively. agr, accessory gene regulatory; CoNS, coagulase-negative *Staphylococcus*.

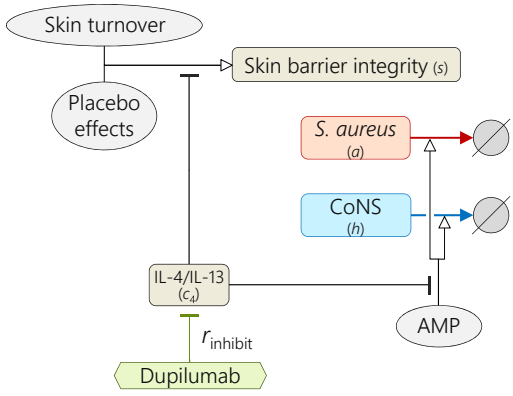

Supplementary Figure S11. Effects of dupilumab. Squared, oval, and hexagon symbols represent model variables, implicit factors, and treatment in our model, respectively. AMP, antimicrobial peptide; CoNS, coagulase-negative *Staphylococcus*.

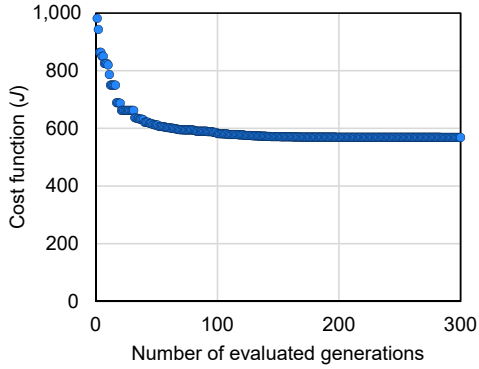

Supplementary Figure S12. The cost function (*J*) reached a plateau value, 569, in the optimization process using differential evolution.

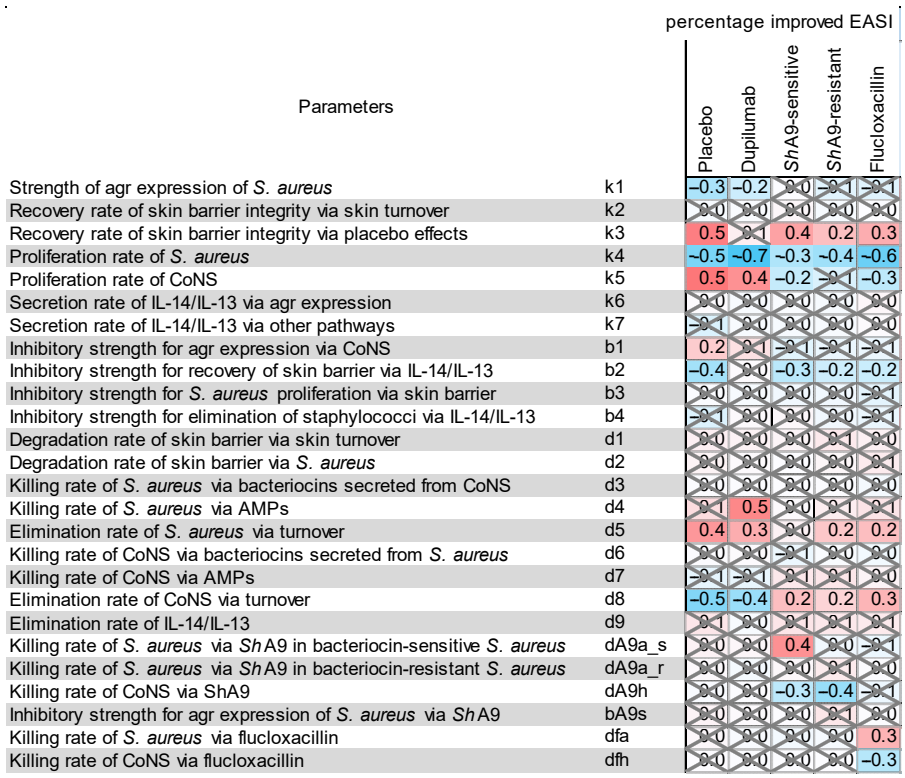

Supplementary Figure S13. PRCC between model parameters and percentage-improved EASI by each treatment. Open and crossed cells are statistically significant and nonsignificant PRCCs (absolute value > 0.1 with adjusted $P < 0.05$), respectively. Positive PRCC means that virtual patients with a higher value of the parameter achieve a higher percentage-improved EASI by the treatment (e.g., k_3). Negative PRCC means that virtual patients with a lower value of the parameter achieve a higher %improved EASI by the treatment (e.g., b_2). agr, accessory gene regulatory; AMP, antimicrobial peptide; CoNS, coagulase-negative *Staphylococcus*; EASI, Eczema Area and Severity Index; PRCC, partial rank correlation coefficient; ShA9, *Staphyloccocus hominis* A9.

Supplementary Table S1. Treatments Excluded in this Study (Except for Antibiotics/Antiseptics)

Treatments	MoA	Clinical Efficacies (Compared with Those of Placebo)	Reasons for Exclusion
Bleach bath (0.005% hypochlorite) (Wong et al., 2013)	Unclear (inhibiting NF-κB?)	Decreased *S. aureus* levels and improved EASI score	Unclear MoA; 0.005% hypochlorite inhibited NF-κB signaling in human keratinocytes but was not antimicrobial against *S. aureus*
Vitreoscilla filiformis Lysate (Gueniche et al., 2008)	Unclear (anti-inflammatory?)	Decreased *S. aureus* levels and improved SCORAD	Unclear MoA: target molecules are unknown
Staphefekt (bacteriophage lysin) (de Wit et al., 2019)	Killing *S. aureus*	Failed to decrease *S. aureus* levels and EASI score compared with placebo	Failed to decrease *S. aureus* levels compared with placebo control
Roseomonas mucosa (Myles et al., 2018)	Producing sphingolipid	Not a placebo-controlled study	Not a placebo-controlled study
Autologous CoNS (Nakatsuji et al., 2021b)	Killing *S. aureus* by bacteriocins	Decreased *S. aureus* levels and improved EASI score	The number of subjects (5–6 subjects/arm) was too small
SRD441 (protease inhibitor) (Foelster et al., 2010)	Inhibiting Staphylococcal-derived aureolysin and matrix metalloproteinases	Slightly improved SCORAD without statistical significance. *S. aureus* levels were not reported	Not reported *S. aureus* levels

Abbreviations: CoNS, coagulase-negative *Staphylococcus*; EASI, Eczema Area and Severity Index; MoA, mechanism of action; SCORAD, scoring atopic dermatitis.

Supplementary Table S2. Biological Factors as Model Variables

Model Variables		Reported Baseline Levels in AD Lesion, Mean (CV)		Range
$c_4(t)$	IL-4/IL-13 level at t	39.2 (55) (Koppes et al., 2016)[1,2]	Fold change against healthy skin	—
$a(t)$	*S. aureus* level at t	3.4 (43) (Nakatsuji et al., 2021a)[3]	Log_{10} CFU/cm^2	0–a_{max}
$h(t)$	CoNS level at t	2.0 (84) (Nakatsuji et al., 2021a)[3]	Log_{10} CFU/cm^2	0–h_{max}
$a_{agr}(t)$	Agr expression level at t	—[4]	—	0 (no effect) ~1 (maximal effect)
$s(t)$	Skin barrier integrity at t	—[4]	—	0 (complete destruction) ~1 (healthy state)
$e(t)$	EASI score at t	29.3 (49) (Blauvelt et al., 2017) [2,3,5]	—	0–72

Abbreviations: AD, atopic dermatitis; agr, accessory gene regulatory; EASI, Eczema Area and Severity Index; CFU, colony-forming unit; CoNS, coagulase-negative *Staphylococcus*; CV, coefficient of variation; IQR, interquartile range.

[1]Patients with mild-to-moderate AD. Values are average of IL-4 (mean = 38.0, CV = 53%) and IL-13 (mean = 40.5, CV = 56).

[2]CV was estimated from IQR.

[3]Patients with moderate-to-severe AD.

[4]No reference data to be compared with simulated values.

[5]Mean baseline value of 29.0 for dupilumab treatment and 29.6 for placebo treatment in dupilumab clinical trial.

Supplementary Table S3. Model Parameters

Parameters		Equations	Explored Range		Selected Values	
			μ_i	σ_i	μ_i	σ_i
k_1	Strength of agr expression	S5	[–2, –1]	[0, 1]	–1.06	0.50
k_2	Recovery rate of skin barrier integrity through skin turnover	S6	[–8, –7]	[0, 1]	–7.71	0.33
k_3	Recovery rate of skin barrier integrity through placebo effects	S6	[–1, 0]	[1, 2]	–0.46	1.58
k_4	Proliferation rate of *S. aureus*	S7	[1–2]	[0, 1]	1.37	0.20
k_5	Proliferation rate of CoNS	S8	[–2, –1]	[0, 1]	–1.26	0.25
k_6	Secretion rate of IL-4/IL-13 through agr expression	S9	[–9, –8]	[2, 3]	–8.10	2.72
k_7	Secretion rate of IL-4/IL-13 through other pathways	S9	[–6, –5]	[0, 1]	–5.02	0.70
b_1	Inhibitory strength for agr expression through CoNS	S5	[1, 2]	[0, 1]	1.37	0.04
b_2	Inhibitory strength for recovery of skin barrier through IL-4/IL-13	S6	[–3, –2]	[0, 1]	–2.67	0.98
b_3	Inhibitory strength for *S. aureus* proliferation through skin barrier	S7	[–7, –6]	[0, 1]	–6.11	0.60
b_4	Inhibitory strength for elimination of *Staphylococci* through IL-4/IL-13	S7, S8	[–3, –2]	[1, 2]	–2.71	1.51
d_1	Degradation rate of skin barrier through skin turnover	S6	[–10, –9]	[1, 2]	–9.86	1.41
d_2	Degradation rate of skin barrier through *S. aureus*	S6	[–9, –8]	[2, 3]	–8.33	2.32
d_3	Killing rate of *S. aureus* by bacteriocins secreted from CoNS	S7	[–5, –4]	[2, 3]	–4.65	2.61
d_4	Killing rate of *S. aureus* by AMPs	S7	[0, 1]	[0, 1]	0.55	0.39
d_5	Elimination rate of *S. aureus* via turnover	S7	[0, 1]	[0, 1]	0.23	0.19
d_6	Killing rate of CoNS via bacteriocins secreted from *S. aureus*	S8	[–9, –8]	[0, 1]	–8.14	0.59
d_7	Killing rate of CoNS via AMPs	S8	[–4, –3]	[1, 2]	–3.44	1.88
d_8	Elimination rate of CoNS through turnover	S8	[–2, –1]	[0, 1]	–1.73	0.40
d_9	Elimination rate of IL-4/IL-13	S9	[–9, –8]	[1, 2]	–8.62	1.19
d_{A9a_s}	Killing rate of *S. aureus* through *Sh*A9 in bacteriocin–sensitive *S. aureus*	S13	[1, 2]	[0, 1]	1.09	0.90
d_{A9a_r}	Killing rate of *S. aureus* through *Sh*A9 in bacteriocin–resistant *S. aureus*	S13	[–1, 0]	[0, 1]	–0.83	0.85
d_{A9h}	Killing rate of CoNS by *Sh*A9	S11	[0, 1]	[0, 1]	0.55	0.90
b_{A9s}	Inhibitory strength for agr expression through *Sh*A9	S12	[–2, –1]	[0, 1]	–1.11	0.27
d_{fs}	Killing rate of S. aureus by flucloxacillin	S14	[0, 1]	[0, 1]	0.13	0.27
d_{fh}	Killing rate of CoNS by flucloxacillin	S15	[0, 1]	[0, 1]	0.35	0.12

Abbreviations: agr, accessory gene regulatory; AMP, antimicrobial peptide; CoNS, coagulase-negative *Staphylococcus*; ShA9, *Staphyloccocus hominis* A9.